

Infrared identification of high-mass X-ray binaries discovered by INTEGRAL

A. Coleiro, S. Chaty, J. A. Zurita Heras, F. Rahoui, J. A. Tomsick

▶ **To cite this version:**

A. Coleiro, S. Chaty, J. A. Zurita Heras, F. Rahoui, J. A. Tomsick. Infrared identification of high-mass X-ray binaries discovered by INTEGRAL. Astronomy and Astrophysics - A&A, 2013, 560, pp.A108. 10.1051/0004-6361/201322382 . cea-01135500

HAL Id: cea-01135500

https://cea.hal.science/cea-01135500

Submitted on 25 Mar 2015

HAL is a multi-disciplinary open access archive for the deposit and dissemination of scientific research documents, whether they are published or not. The documents may come from teaching and research institutions in France or abroad, or from public or private research centers.

L'archive ouverte pluridisciplinaire **HAL**, est destinée au dépôt et à la diffusion de documents scientifiques de niveau recherche, publiés ou non, émanant des établissements d'enseignement et de recherche français ou étrangers, des laboratoires publics ou privés.

A&A 560, A108 (2013)
DOI: 10.1051/0004-6361/201322382
© ESO 2013

Astronomy & Astrophysics

Infrared identification of high-mass X-ray binaries discovered by INTEGRAL⋆

A. Coleiro[1], S. Chaty[1,2], J. A. Zurita Heras[3], F. Rahoui[4,5], and J. A. Tomsick[6]

[1] Laboratoire AIM (UMR-E 9005 CEA/DSM – CNRS – Université Paris Diderot), Irfu/Service d'Astrophysique, CEA-Saclay, 91191 Gif-sur-Yvette Cedex, France
e-mail: alexis.coleiro@cea.fr
[2] Institut Universitaire de France, 103 Boulevard Saint Michel, 75006 Paris, France
[3] François Arago Centre, APC, Université Paris Diderot, CNRS/IN2P3, CEA/Irfu, Observatoire de Paris, Sorbonne Paris Cité, 10 rue Alice Domon et Léonie Duquet, 75205 Paris Cedex 13, France
[4] European Southern Observatory, Karl Schwarzschild-Strasse 2, 85748 Garching bei München, Germany
[5] Department of Astronomy, Harvard University, 60 Garden Street, Cambridge, MA 02138, USA
[6] Space Science Laboratory, 7 Gauss Way, University of California, Berkeley, CA 94720-7450, USA

Received 27 July 2013 / Accepted 13 September 2013

ABSTRACT

Context. Since it started observing the sky, the INTEGRAL satellite has discovered new categories of high mass X-ray binaries (HMXB) in our Galaxy. These observations raise important questions on the formation and evolution of these rare and short-lived objects.
Aims. We present here new infrared observations from which to reveal or constrain the nature of 15 INTEGRAL sources, which allow us to update and discuss the Galactic HMXB population statistics.
Methods. After previous photometric and spectroscopic observing campaigns in the optical and near-infrared, new photometry and spectroscopy was performed in the near-infrared with the SofI instrument on the ESO/NTT telescope in 2008 and 2010 on a sample of INTEGRAL sources. These observations, and specifically the detection of certain features in the spectra, allow the identification of these high-energy objects by comparison with published NIR spectral atlases of O and B stars.
Results. We present photometric data of nine sources (IGR J10101-5654, IGR J11187-5438, IGR J11435-6109, IGR J14331-6112, IGR J16328-4726, IGR J17200-3116, IGR J17354-3255, IGR J17404-3655, and IGR J17586-2129) and spectroscopic observations of 13 sources (IGR J10101-5654, IGR J11435-6109, IGR J13020-6359, IGR J14331-6112, IGR J14488-5942, IGR J16195-4945, IGR J16318-4848, IGR J16320-4751, IGR J16328-4726, IGR J16418-4532, IGR J17354-3255, IGR J17404-3655, and IGR J17586-2129). Our spectroscopic measurements indicate that: five of these objects are Oe/Be high-mass X-ray binaries (BeHMXB), six are supergiant high-mass X-ray binaries (sgHMXB), and two are sgB[e]. From a statistical point of view, we estimate the proportion of confirmed sgHMXB to be 42% and that of the confirmed BeHMXB to be 49%. The remaining 9% are peculiar HMXB.

Key words. supergiants – stars: fundamental parameters – X-rays: binaries – infrared: stars – binaries: general

1. Introduction

The INTEGRAL observatory has been observing the sky for ten years. By performing a detailed survey of the Galactic plane, it has discovered numerous new hard X-ray binary candidates that need to be identified. Of these, numerous high-mass X-ray binaries (HMXB) have been identified previously.

HMXB are interacting binary systems composed of a compact object orbiting around an O/B high-mass star. They are mainly located close to their formation sites in the Galactic plane (see e.g. Bodaghee et al. 2012; Coleiro & Chaty 2013). These sources are typically separated into two principal families: Be X-ray binaries (BeHMXB) which consist of a neutron star that accretes matter when it moves through the equatorial decretion disk of a Be star, and supergiant X-ray binaries (sgHMXB), for which the donor object is an O/B supergiant star that feeds the compact object via its intense stellar wind. In this last category, studied by Lutovinov et al. (2013), appear two subclasses of binary systems that were previously undetected. The first one consists in intrinsically highly obscured (with column densities $N_{\rm H}$ higher than about 10^{23} cm^{-2}) hard X-ray sources, the most extreme example of which is the source IGR J16318-4848 (Chaty & Rahoui 2012). The second one is composed of compact objects associated with a supergiant donor that undergo fast and transient outbursts in the X-ray domain of the electromagnetic spectrum. These latter sources are called supergiant fast X-ray transients (SFXT; Negueruela et al. 2006), which represented by their archetype, IGR J17544-2619 (Pellizza et al. 2006).

Owing to their high intrinsic extinction and to interstellar absorption in the Galactic plane, detecting HMXB in longer wavelengths is challenging but crucial for any further study of their nature. In this context, near-infrared (NIR) observations appear to be very efficient in determining the nature of these HMXB by constraining the spectral type of the companion star.

In this article, we present results of an intensive NIR study of a sample of candidate HMXB for which an accurate X-ray

⋆ Based on observations carried out at the European Southern Observatory (La Silla, Chile) under program IDs 080.D-0864(A) and 084.D-0535(A).

Table 1. X-ray position, uncertainty for the observed X-ray sources, and galactic longitude (l), and latitude (b).

Source	RA	Dec	Unc.	l	b	Photometry	Spectroscopy
IGR J10101-5654	10:10:11.87	–56:55:32.1	0.″64 (*Chandra*)	282.2568	–00.6721	yes	yes
IGR J11187-5438	11:18:21.1	–54:37:32.0	3.″7 (*Swift*)	289.6400	5.8260	yes	no
IGR J11435-6109	11:44:00.31	–61:07:36.5	0.″64 (*Chandra*)	294.8815	0.6865	yes	yes
IGR J13020-6359	13:01:59.2	–63:58:06.0	3.″5 (*Swift*)	304.0892	–1.1203	yes	yes
IGR J14331-6112	14:33:08.33	–61:15:39.9	0.″64 (*Chandra*)	314.8463	–0.7642	yes	yes
IGR J14488-5942	14:48:43.3	–59:42:16.3	3.″7 (*Swift*)	317.2340	–0.1298	yes	yes
IGR J16195-4945	16:19:32.20	–49:44:30.7	0.″6 (*Chandra*)	333.5570	0.3390	yes	yes
IGR J16318-4848	16:31:48.6	–48:49:00	4″ (XMM)	335.6167	–0.4482	yes	yes
IGR J16320-4751	16:32:01.9	–47:52:27	3″ (XMM)	336.3300	0.1689	yes	yes
IGR J16328-4726	16:32:37.88	–47:23:42.3	1.″7 (*Swift*)	336.7491	0.4220	yes	yes
IGR J16418- 4532	16:41:50.65	–45:32:27.3	1.″9 (*Swift*)	339.1883	0.4889	yes	yes
IGR J17200-3116	17:20:05.92	–31:16:59.4	0.″64 (*Chandra*)	355.0222	3.3474	yes	no
IGR J17354-3255	17:35:27.59	–32:55:54.4	0.″64 (*Chandra*)	355.4576	–0.2730	yes	yes
IGR J17404-3655	17:40:26.86	–36:55:37.4	0.″64 (*Chandra*)	352.6259	–3.2725	yes	yes
IGR J17586-2129	17:58:34.56	–21:23:21.6	0.″64 (*Chandra*)	7.9862	1.3266	yes	yes

Notes. Observing mode(s) (photometry and/or spectroscopy) are also given for each source.

Table 2. Counterpart position and photometry results from this study.

Source	RA	Dec	Obs. date	AM	ET	J mag.	H mag.	K_s mag.
			2008 Run					
IGR J11187-5438	11:18:21.21	–54:37:28.6	2008-03-09T07:08:39.930	1.2	10.0	15.66 ± 0.04	14.99 ± 0.02	14.68 ± 0.02
IGR J11435-6109	11:44:00.3	–61:07:36.5	2008-03-09T05:54:12.202	1.2	10.0	12.90 ± 0.02	12.23 ± 0.02	11.77 ± 0.02
IGR J17200-3116	17:20:06.1	–31:17:02.0	2008-03-09T08:35:06.750	1.1	10.0	13.50 ± 0.02	12.48 ± 0.02	12.04 ± 0.02
			2010 Run					
IGR J10101-5654	10:10:11.87	–56:55:32.1	2010-03-29T01:17:11.318	1.2	2.0	–	–	10.742 ± 0.02
IGR J14331-6112	14:33:08.33	–61:15:39.7	2010-03-28T04:53:33.431	1.3	10.0	–	–	13.691 ± 0.02
IGR J16328-4726	16:32:37.91	–47:23:40.9	2010-03-29T07:45:12.428	1.1	10.0	–	–	11.309 ± 0.02
IGR J17354-3255	17:35:27.60	–32:55:54.40	2010-03-30T06:51:03.000	1.3	10.0	–	–	10.395 ± 0.02
IGR J17404-3655	17:40:26.85	–36:55:37.6	2010-03-30T08:10:58.684	1.1	10.0	–	–	14.370 ± 0.02
IGR J17586-2129	17:58:34.56	–21:23:21.53	2010-03-30T07:44:31.981	1.2	2.0	–	–	9.4

Notes. We point out that the K_s-band magnitude of IGR J17586-2129 is not accurate since photometric data of this source were saturated. Airmass (AM) and single exposure time in seconds (ET) are also given for each source.

localization is available. In Sect. 2 we describe the ESO NIR photometric and spectroscopic observations along with our data reduction strategy. In Sect. 3 we review previously published properties of each source before reporting the results of our NIR observations. Finally, we discuss the results of the observations and implications in Sect. 4 before concluding.

2. Observations and analysis

The observations are based on astrometry, photometry, and spectroscopy of the 15 INTEGRAL sources listed in Table 1. They were carried out on 2008 March 07–09 and 2010 March 27–29 at the European Southern Observatory (ESO, Chile), in NIR (1–2.5 μm) using the SofI instrument installed on the 3.5 m New Technology Telescope (NTT) at the La Silla observatory. These observations were performed through ESO programs ID 080.D-0864(A) and 084.D-0535 (PI Chaty), in visitor mode.

2.1. Photometry

We performed NIR photometry in the J-, H-, and K_s-bands of the sources listed in Table 2. We used the large field of SofI's detector, giving an image scale of 0.″288/pixel and a field of view of 4.′92 × 4.′92. The photometric observations were obtained by repeating a set of images for each filter with nine different 30″ offset positions including the targets, following the standard jitter procedure, which enabled us to cleanly subtract the sky emission in NIR. Each individual frame has an integration time of 10 s, giving a total exposure time of 90 s in each energy band. Moreover, three photometric standard stars chosen in Persson's catalog (Persson et al. 1998) were observed in the three bands with a total integration time of 10 s for each target in each band.

We used the Image Reduction and Analysis Facility (IRAF) suite[1] to perform data reduction and carry out standard proce-

[1] IRAF is distributed by the National Optical Astronomy Observatories, which are operated by the Association of Universities for Research in Astronomy, Inc., under cooperative agreement with the National Science Foundation.

Table 3. Log of NIR spectra.

Source	Obs. date	AM	ET	Filter	Slit width
IGR J10101-5654	2010-03-28T00:21:11.7584	1.2	60.0	K_s	0.″6
″	2010-03-30T00:22:04.8787	1.2	60.0	H	1.″0
IGR J11435-6109	2010-03-29T02:37:37.6419	1.2	60.0	K_s	0.″6
″	2010-03-30T02:37:54.2772	1.2	60.0	H	1.″0
IGR J13020-6359	2010-03-29T03:35:41.7071	1.3	60.0	K_s	1.″0
IGR J14331-6112	2010-03-28T05:08:59.2288	1.2	60.0	K_s	1.″0
IGR J14488-5942	2010-03-29T05:56:02.3304	1.2	60.0	K_s	1.″0
IGR J16195-4945	2010-03-30T04:42:57.4456	1.5	60.0	K_s	1.″0
″	2010-03-30T03:59:32.1327	1.7	60.0	H	1.″0
IGR J16318-4848	2010-03-28T05:51:33.3738	1.3	60.0	K_s	0.″6
IGR J16320-4751	2010-03-28T06:37:01.7617	1.2	60.0	K_s	1.″0
IGR J16328-4726	2010-03-29T08:03:29.7491	1.1	60.0	K_s	1.″0
IGR J16418-4751	2010-03-28T07:31:53.0447	1.1	60.0	K_s	1.″0
IGR J17354-3255	2010-03-30T07:05:38.8785	1.2	60.0	K_s	1.″0
IGR J17404-3655	2010-03-30T08:31:51.5539	1.1	60.0	K_s	1.″0
IGR J17586-2129	2010-03-30T07:56:13.1784	1.2	5.0	K_s	1.″0

Notes. The name of the source, the date and UT time of the observations, the airmass (AM), the exposure time in seconds (ET), the filter and the slit width are indicated. All spectra were obtained at ESO/NTT with SofI instrument.

dures of NIR image reduction, including flat-fielding and NIR sky subtraction.

We performed accurate astrometry on each entire SofI 4.′92 × 4.′92 field, using all stars from the 2MASS catalog in this field. The rms of the astrometry fit was always lower than 0.″6.

We carried out aperture photometry on photometric standard stars and computed the zero-point value for each energy band knowing the instrumental magnitudes and the apparent magnitudes (given in Persson's catalog) and using the standard relation $\mathrm{mag_{app}} = \mathrm{mag_{inst}} - \mathrm{Zp}$, where $\mathrm{mag_{app}}$ and $\mathrm{mag_{inst}}$ are the apparent and instrumental magnitudes, respectively, and Zp is the zero-point, including the extinction and airmass terms. After computing the zero-point value for each filter, we performed PSF-fitting photometry on the crowded fields that contained the six sources under study following the standard utilization of the IRAF *noao.digiphot.daophot* package. After evaluating an aperture correction for each filter and each object (due to the difference of aperture radius used to perform photometry on standard stars and targets) and knowing the zero-point values, we derived the apparent magnitude of the targets in the three NIR filters. The results are given in Table 2.

2.2. Spectroscopy

We also carried out NIR spectroscopy with SofI. In 2008, low-resolution spectra were obtained between 1.53 and 2.52 μm, but, spectra are not presented in this paper because of the low signal-to-noise ratio (S/N) that was caused by bad weather which prevented us from extracting any useful data. In 2010, we used the medium-resolution grism with H and K_s filters (properties of the grisms are given in Table 4). For each source, eight spectra were taken with both filters, half of them with the 1.″0 (or 0.″6) slit on the source and the other half with an offset of 30″, in order to subtract the NIR sky emission. Each individual spectrum has an exposure time of 60 s, giving a total integration time of 480 s. Furthermore, four telluric standards were observed immediately after each target with the same instrument set-up and a total integration time of 8 s. A summary of the spectroscopic observations is provided in Table 3.

We analyzed the NIR spectra using standard IRAF tasks, correcting for flat field, removing the crosstalk, correcting the geometrical distortion, combining the images and finally extracting the spectra and performing wavelength calibration using the IRAF *noao.twodspec* package. Wavelength calibration was made with a Xenon lamp which presents a good distribution of lines and is sufficient to calibrate data taken with the low-resolution grisms of the SofI instrument. The target spectra were then corrected for the telluric lines using the standard stars observed with the same configuration.

3. Results

All sources studied in this paper were discovered with the IBIS/ISGRI detector onboard the INTEGRAL observatory. Furthermore, they were all observed with other X-ray facilities to provide an accurate localization, which allowed us to determine the optical/NIR counterpart. The sample of 15 sources is given in Table 1. We present below our results on each source, for which we followed the same strategy. We first observed the field in NIR, performed accurate astrometry, and derived the photometry of the counterpart candidate for most of them. We then analyzed the NIR spectrum.

We also underline that the low S/N and the medium-resolution of the spectra prevent a quantitative study. Moreover, important lines such as He I at 2.058 μm and Brγ at 2.1661 μm are often subject to difficulties because of the strong telluric absorption present at these wavelengths. Thus, considering these issues, we mostly conducted a qualitative analysis based on a comparison of our NIR spectra with available NIR spectral atlases (Hanson et al. 1996, 2005; Morris et al. 1996; McGregor et al. 1988; Clark et al. 1999; Steele & Clark 2001). In general, we considered as a stellar line (and not a spurious feature) each line detected at least at 3σ of the noise estimated locally, that had a width broader than the instrumental width of 20 Å for the H filter and 18 Å for the K_s filter with the 1.″0 slit.

Table 4. Wavelength range and resolution for each grism.

Filter name	Wavelength range (microns)	Slit width	Resolving power	Dispersion (Å/pixel)
H	1.50–1.80	1.″0	900	3.43
H	1.50–1.80	0.″6	1500	3.43
K_s	2.00–2.30	1.″0	1320	4.62
K_s	2.00–2.30	0.″6	2200	4.62

Notes. The resolution is given for the 1.″0 and 0.″6 slit respectively.

Each detected line was fitted by a Gaussian profile using the IRAF *splot* task. We list its fitted position $\lambda_{\rm fit}$, its equivalent width (EW), its full width at half maximum (FWHM), and its flux in Table 5. We estimate the average error on these parameters to be 20% because of the noise and localization of the continuum. Finally, according to the resolution of the instrument, we considered that a feature can be offset from its laboratory rest wavelength. This offset $\Delta\lambda$ (computed for the 1.″0 slit and approximated by $\Delta\lambda = \lambda/R$, where R is the resolving power given in Table 4) can be as large as 20 Å for the H filter and 18 Å for the K_s filter.

3.1. IGR J10101-5654

IGR J10101-5654 was discovered on 2006 January by Kuiper et al. (2006) with the instrument IBIS ISGRI at the position RA = $10^h10^m07\overset{s}{.}8$, Dec = –56°54′46.″4 (equinox J2000.0; uncertainty 2.″2). Masetti et al. (2006a) localized an optical counterpart at RA = $10^h10^m11\overset{s}{.}866$, Dec = –56°55′32.″06 (equinox J2000.0; accuracy better than 0.″1) and the optical spectrum is typical of an HMXB optical counterpart, showing strong narrow Hα emission superimposed on a reddened continuum. The lack of reliable optical photometry for this counterpart prevented them from deriving a spectral type for this object. Nevertheless, the Hα EW value appears too high for a supergiant star. Thus, the authors suggest that this HMXB hosts a secondary star of intermediate luminosity class (early giant). Tomsick et al. (2008) confirmed the counterpart suggested by Masetti et al. (2006a). Their *Chandra* spectrum also gives a column density of $N_{\rm H} = 3.2^{+1.2}_{-1.0} \times 10^{22}$ cm^{-2} and does not indicate a high level of local absorption. The *Chandra* flux, extrapolated into the 20–40 keV INTEGRAL band, appears to be significantly lower than the flux measured by INTEGRAL (flux ratio of 0.05 ± 0.04). This indicates an important change in mass accretion rate onto the compact object and could be explained by an eccentric binary orbit (Tomsick et al. 2008). *Swift* observations analyzed by Rodriguez et al. (2009) finally confirmed the previously suggested association for this object, that it is very likely an HMXB and also the possible substantial variation of the mass accretion rate.

NIR spectra of the source are shown in Fig. 1. We report the detected lines in Table 5. The H-band spectrum exhibits the Brackett series from Br(20–4) line at 1.5198 μm to the Br(10–4) transition at 1.7377 μm. Two lines could match the position of [Fe II] lines at 1.6427 μm and 1.7122 μm (this hypothesis is discussed at the end of the paragraph). The K_s-band spectrum clearly shows He I at 2.0586 μm and Br(7–4) at 2.1659 μm. Mg II, He II, Na I, and Fe II emission lines are also detected in this spectrum. The NIR spectra are typical of a Be companion star and the intensity ratio of the Br(7–4) and He I (at 2.0586 μm) lines suggests a B0.5Ve or a B0Ivpe type (Hanson et al. 1996). However, the [Fe II] emission lines are confusing. Indeed, these forbidden lines are typical of the B[e] phenomenon and are tracers of recombination in a dense stellar wind (Clark et al. 1999). The Na I emission line suggests the presence of a low-excitation region that is not directly exposed to the radiation of the star or the compact object. It is probably the signature of an extended circumbinary envelope (McGregor et al. 1988). A feature at 2.1226 μm might be associated with the molecular hydrogen H_2 ro-vibrational $v = 1$–0, $J = 3$–1 S(1) emission line. If this feature is real, its presence and that of [Fe II] lines could trace supersonic shocks that heat the gas (see e.g. Clark et al. 1999; Chen et al. 1998). These processes are very similar to those generally observed in the close environment of young stellar objects (YSOs; see e.g. Chen et al. 1998). Finally, the He I line at 2.058 μm shows a double-peaked shape. The separation is $c\frac{\Delta\lambda}{\lambda} = 290$ km s^{-1}, larger than the resolution of the instrument, $c\frac{\Delta\lambda}{\lambda} \sim 260$ km s^{-1}. While this double-peak structure could be the signature of a circumstellar disk, this result remains uncertain. Then we suggest that this source is surrounded by a highly stratified environment composed of regions shielded from the direct stellar radiation.

Moreover, we fitted the spectral energy distribution (SED) from optical to mid-infrared (MIR) wavelengths[2] with a model that combines two absorbed blackbodies (see Fig. 5), one representing the companion star emission and another one representing a possible MIR excess due to absorbing material that enshrouds the companion star (see e.g. Rahoui et al. 2008). The free parameters of the fits are the absorption in V band, A_V, the radius-to-distance ratio R_*/D, the additional blackbody component temperature $T_{\rm d}$, and its radius $R_{\rm d}$. The stellar blackbody temperature is fixed to 20 000 K. The best-fitting parameters are $A_V = 13.1 \pm 0.86$ mag, $R/D = 2.79 \pm 0.20\ R_\odot$/kpc, $T_{\rm d} = 1016$ K ± 127, $R_{\rm d}/D = 28.3 \pm 4.25\ R_\odot$/kpc, and χ^2/d.o.f. = 2.23. For comparison, the best-fitting parameters without the additional component are $A_V = 17.01 \pm 0.46$ mag, $R/D = 3.86 \pm 0.09\ R_\odot$/kpc, and χ^2/d.o.f. = 23.58.

To conclude, SED fitting shows a clear MIR excess, most likely caused by the presence of warm dust around the system. Moreover, NIR spectra of IGR J10101-5654 present many similarities with stars that show the B[e] phenomenon, even though the optical spectrum of this source, published by Masetti et al. (2006a), appears to be very different from the optical spectrum expected for a B[e] phenomenon. Indeed, we can reasonably assume that in the optical spectrum, one mainly detects radiation from the stellar photosphere whereas the NIR spectra mostly probes the circumstellar environment, which is characterized by a B[e] phenomenon. We suggest that IGR J10101-5654 is a supergiant B[e]. Figure 6 compares the K_s spectrum of the source with K_s spectra of IGR J11435-6109 and IGR J13020-6359.

[2] We note that B and R magnitudes, coming from the USNO survey seem to be unreliable. Because of the faintness of the source in the optical, we did not take optical magnitudes into account in the fitting procedure.

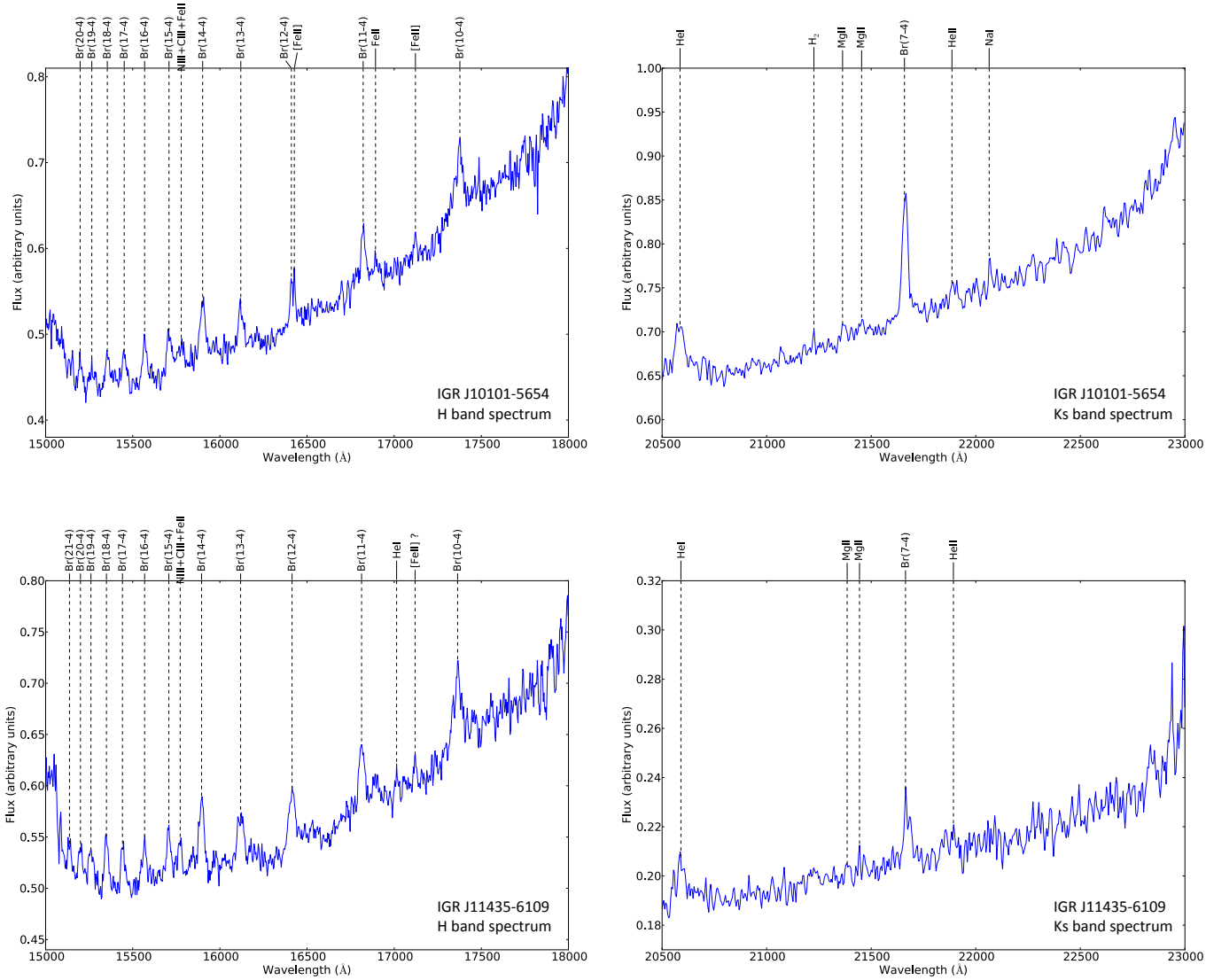


Fig. 1. Spectra of IGR J10101-5654 (H-band: *top left* and K_s-band: *top right*), and IGR J11435-6109 (H-band: *bottom left* and K_s-band: *bottom right*).

These spectra seem very similar but the Brγ emission line of IGR J10101-5654 looks broader than those of the last two.

3.2. IGR J11187-5438

IGR J11187-5438 was discovered by Bird et al. (2007) at the position RA = $11^h18^m21\overset{s}{.}1$, Dec = –54°37′32″ (equinox J2000.0; uncertainty 4′). Rodriguez et al. (2008) conducting *Swift* observations refined the position of the source and found a single source in the 2MASS catalog (2MASS J11182121-5437286) that is also visible in the DSS II catalog. The 0.5–9 keV spectrum is well fitted by an absorbed power law with $\Gamma = 1.5$ and $N_H = 0.28 \times 10^{22}$ cm^{-2} similar to the Galactic absorption along the line of sight meaning that the source is not intrinsically absorbed.

We fitted the SED, constituted by the I, J, H, K_s, WISE 3.4, and WISE 4.6 band magnitudes (see Table 8), with a stellar blackbody model with three free parameters: the companion star temperature T, the ratio radius of the companion star over the distance, R/D, and the extinction in the V band A_V. The retrieved parameters are not consistent with early star parameter values: $A_V = 3.9 \pm 0.4$ mag, $T = 6000$ K, $R/D = 0.60 \pm 0.03$ $R_\odot$/kpc, and χ^2/d.o.f. = 3.45 (see Fig. 5). Thus, this source is probably not an HMXB but it might be a low mass X-ray binary (LMXB).

3.3. IGR J11435-6109

IGR J11435-6109 was discovered by Grebenev et al. (2004) at the position RA = $11^h43^m52^s$, Dec = –61°09′00″, (equinox J2000.0; uncertainty 2′.5). The optical and infrared counterparts were discovered by Tomsick et al. (2007) and confirmed by Negueruela et al. (2007) as 2MASS J11440030-6107364 = USNO-B1.0 0288-0337502. *Beppo*SAX-WFC observations carried out by in't Zand & Heise (2004) and Swank & Markwardt (2004) suggested a column density of $N_H \sim 9 \times 10^{22}$ cm^{-2} and a Γ value of ∼1.9–2.3. These values were confirmed by Tomsick et al. (2008) who fitted the *Chandra*/ACIS spectrum with a power-law and found an N_H value of 15×10^{22} cm^{-2} and a Γ value of ∼1.1. in't Zand & Heise (2004) detected a pulsation of 161.76 ± 0.01 s and a possible orbital period of 52.5 days which was confirmed by Corbet & Remillard (2005) and Wen et al. (2006) with *RXTE/ASM* observations that gave an orbital period of 52.46 ± 0.06 days and 52.36 days respectively. Tomsick et al. (2007), thanks to *Chandra* observations, concluded that

IGR J11435-6109 is an HMXB with a significant amount of intrinsic absorption. This result was confirmed by optical observations of the source, conducted by Negueruela & Schurch (2007): the source is not detected below 5000 Å whereas the 5000–7800 Å spectrum shows a strong Hα emission line on top of a reddened continuum. The equivalent width of the Hα line is equal to –26 Å, and the lack of other stellar features enabled them to classify the companion star as an obscured Be star, compatible with the position of the system in the Corbet diagram (Corbet & Remillard 2005). Finally, the spectral type was constrained by Masetti et al. (2009) who suggested a B2III or B0V counterpart with an extinction A_V of 5.7.

The NIR spectra of the source are shown in Fig. 1. We report the detected lines in Table 5. The H-band spectrum exhibits the Brackett series from the Br(21–4) line at 1.5137 μm to the Br(10–4) transition at 1.7364 μm. An additional line may match with the position of [Fe II] line at 1.7120 μm and another one, located at 1.7014 μm, may match with an He I line. N III, C III and Fe II may also be detected around 1.5772 μm. The K_s band spectrum clearly shows He I at 2.0590 μm and Br(7–4) at 2.1664 μm. Mg II and He II emission lines are also present in this spectrum. The NIR spectra are pretty similar to those of IGR J10101-5654 but fewer lines are detected. Especially some typical lines of stars that exhibit B[e] phenomenon are not observed. Thus, we consider these spectra typical of a Be companion star and the intensity ratio of the Br(7–4) and He I (at 2.0590 μm) lines suggests a B0.5Ve (Hanson et al. 1996) (see comparison spectra in Fig. 6, left panel). Moreover, we fitted the SED from optical to MIR wavelengths[3] with a model that combines two absorbed blackbodies (see Fig. 5), one representing the companion star emission and another one representing a possible MIR excess due to absorbing material enshrouding the companion star (see e.g. Rahoui et al. 2008). The free parameters of the fits are the absorption in V band, A_V, the radius-to-distance ratio R_*/D, the additional blackbody component temperature T_d and its radius R_d. The stellar blackbody temperature was fixed to 20 000 K. The best-fitting parameters are $A_V = 7.98 \pm 0.44$ mag, $R/D = 1.33 \pm 0.05$ $R_\odot$/kpc, $T_d = 925.6$ K ± 190.7, $R_d/D = 51.6 \pm 2.97$ $R_\odot$/kpc, χ^2/d.o.f. = 1.14. For comparison, the best-fitting parameters without the additional component are $A_V = 8.98 \pm 0.18$ mag, $R/D = 1.46 \pm 0.03$ $R_\odot$/kpc, and χ^2/d.o.f. = 6.81. Thus SED fitting shows a relatively weak MIR excess, which we consider to be probably due to bremsstrahlung emission coming from the decretion disk of a Be star. Thus, we confirm the Be type of this HMXB and constrain its spectral type to B0.5Ve.

3.4. IGR J13020-6359

IGR J13020-6359 was discovered in 2006 by Bird et al. (2006) and was classified as a pulsar/HMXB in Bird et al. (2007) based on its position coinciding with 2RXP J130159.6–635806 studied by Chernyakova et al. (2005) who conducted multi-epoch ASCA, *Beppo*SAX, *XMM-Newton* and INTEGRAL observations. The observed long term behaviour and the spectral and timing properties tend to indicate a HMXB with Be companion. These authors identified a probable 2MASS infrared counterpart at (RA, Dec J2000.0) = ($13^h01^m58\overset{s}{.}7$, –63°58′09″). The *Swift* spectrum, well fitted with a power law, shows some slight variability as expected for an accreting pulsar (Rodriguez et al. 2009) optical spectroscopy carried out by Masetti et al. (2006b), constrained the spectral type of the companion star to B1III or O9V.

The K_s-band spectrum of the source is shown in Fig. 2. We report the detected lines in Table 5. This spectrum clearly shows the He I at 2.0594 μm and Br(7–4) at 2.1663 μm. Even though no other lines are detected, the NIR spectrum is typical of a Be companion star and the intensity ratio of the Br(7–4) and He I (at 2.0594 μm) lines suggests a B0.5Ve or a B0Ivpe type (Hanson et al. 1996), similar to IGR J10101-5654 and IGR J11435-6109 (see Fig. 6, left panel). We therefore confirm the Be type of this HMXB and constrain its spectral type to B0.5Ve.

3.5. IGR J14331-6112

IGR J14331-6112 was discovered in 2006 by Keek et al. (2006) at the position (RA, Dec J2000.0) = ($14^h33^m06\overset{s}{.}2$, –61°12′23″, $3\overset{\prime}{.}9$ uncertainty). Landi et al. (2007) obtained a *Swift* position and detected a possible USNO-B1.0 counterpart, allowing Masetti et al. (2008) to carry out optical spectroscopy. From this, the authors suggested the source to be an HMXB hosting a companion star with a BIII or a BV spectral type. Finally, *Chandra* observations conducted by Tomsick et al. (2009) confirmed the identification of the system and showed that the *Chandra* energy spectrum is well fitted with an absorbed power law with a column density value $N_H = 2.2^{+0.9}_{-0.8} \times 10^{22}$ cm^{-2} and a photon index $\Gamma = 0.34^{+0.37}_{-0.33}$. Moreover, a very strong iron Kα-emission line is detected with an equivalent width of ~945 eV. A possible existence of a soft excess is related.

The K_s band spectrum of the source is shown in Fig. 2. We report the detected lines in Table 5. Even though the S/N of this spectrum is low, it shows the Br(7–4) emission line at 2.1657 μm. Moreover, assuming that the Brγ emission line is mainly detected in supergiant and Be stars (hardly ever in main-sequence stars), and knowing that in supergiant star spectra, He I at 2.058 μm in emission is generally detected as well, we argue that IGR J14331-6112 could be a Be star, since we do not detect this emission line. Thus, while we cannot conclude definitively on the spectral type of the companion star of IGR J14331-6112, it is probably a Be star, according to the presence of the Br(7–4) emission line.

3.6. IGR J14488-5942

IGR J14488-5942 was first mentioned by Bird et al. (2010) as a transient source. Two X-ray sources are detected in the INTEGRAL/IBIS error circle by Landi et al. (2009) and during *Swift* observations by Rodriguez et al. (2010). Both seem to be Galactic sources but the authors were unable to further confirm which of these two sources was the true counterpart of the INTEGRAL detection. Both Landi et al. (2009) and Rodriguez et al. (2010) suggest that *Swift* J144843.3-594216 is the true INTEGRAL/IBIS counterpart. 2MASS J14484322-5942137 seems to be the NIR counterpart with $J = 15.46$, $H = 13.53$ and $K_s = 12.43$. Its *Swift*/XRT spectrum is well fitted with an absorbed power law spectrum, with N_H value of 1.3×10^{23} cm^{-2}, a photon index of ~3 according to Landi et al. (2009) and Rodriguez et al. (2010). Finally, Corbet et al. (2010b) analyzed the 15–100 keV light curve of this source and detected a highly significant modulation at a period near 49 days. This long term variation is interpreted as the orbital period of an HMXB (possibly a BeHMXB).

[3] We note that B and R magnitudes, coming from the USNO survey seem to be unreliable. Because of the faintness of the source in the optical, we did not take optical magnitudes into account in the fitting procedure.

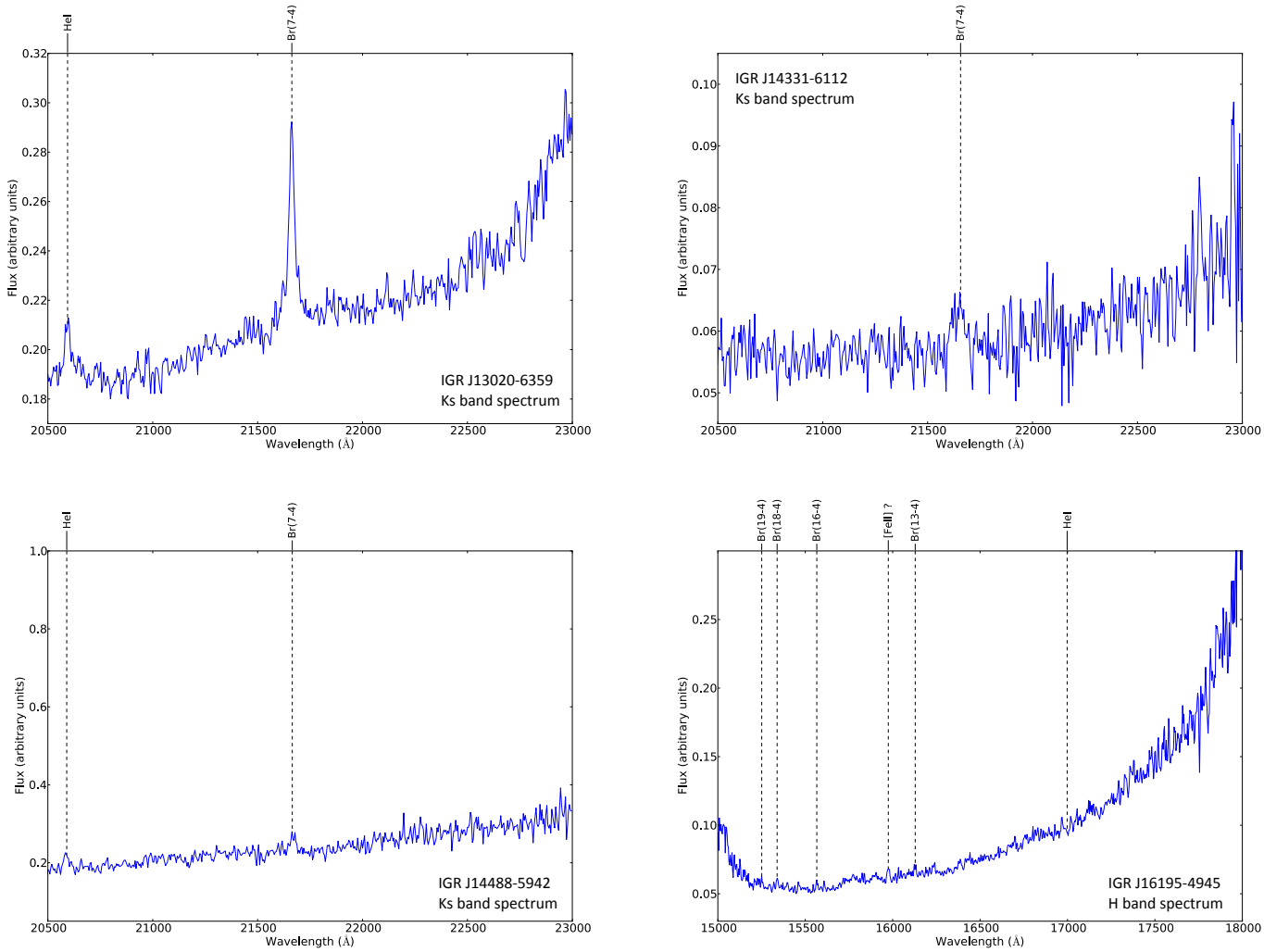


Fig. 2. Spectra of IGR J13020-6359 (*top left*), IGR J14331-6112 (*top right*), IGR J14488-5942 (*bottom left*), and IGR J16195-4945 (*bottom right*, *H*-band).

The K_s-band spectrum of the source (see Fig. 2) only shows potential emission lines of He I at 2.0590 μm and Br(7–4) at 2.1665 μm. All the detected lines are reported in Table 5. We cannot strictly conclude on the spectral type of the companion star but, as far as we know, there is no supergiant star that presents both He I at 2.058 μm and Brγ in emission with the same intensity and the absence of any other feature. On the contrary, Clark et al. 1999 indicates that classical BeHMXB do not usually show evidence for emission from species other than H I and He I, and that the equivalent width of He I at 2.058 μm typically exceeds that of Brγ. Since we only detected H I and He I and because the equivalent width of He I at 2.058 μm is greater than that of Brγ, we conclude that this HMXB is more likely an Oe/Be HMXB than a supergiant one.

3.7. IGR J16195-4945

IGR J16195-4945 was detected with INTEGRAL (**?**). Sidoli et al. (2005), using INTEGRAL observations, derive an average flux of ~17 mCrab in the 20–40 keV band. Follow-up observations conducted by Sguera et al. (2006) showed that the source behaves like an SFXT and reported a peak-flux of ~35 mCrab in the 20–40 keV band. Tomsick et al. (2006), using *Chandra* observations refined the position of the source to 0.″6 accuracy, which allowed them to find the NIR and MIR counterparts in the 2MASS (2MASS J16193220- 4944305) and in the GLIMPSE (G333.5571+00.3390) catalogs. The spectrum is well fitted with an absorbed power law with $\Gamma \sim 0.5$ and $N_{\rm H} \sim 7 \times 10^{22}$ cm^{-2}. According to Tomsick et al. (2006), the SED of the companion star is compatible with an O, B or A supergiant star. A possible USNO counterpart was detected but both Tomsick et al. (2006) and Tovmassian et al. (2006) suggested that the source is blended with a foreground object. Rahoui et al. (2008) did not detect the source in 2006 with VISIR, the MIR instrument on the VLT UT3 telescope. Nevertheless, they fitted its SED using NIR data and the GLIMPSE flux values given in Tomsick et al. (2006). This study revealed that the source exhibits a MIR excess, which is needed to correctly fit the SED. However, this excess is weak and the stellar component is still consistent with an O/B massive star (Rahoui et al. 2008). Finally, Morris et al. (2009), using *Suzaku* observations, revealed a heavily absorbed HMXB and mentioned the possible presence of a disk around the donor star through models of accretion. From theoretical considerations, they can also estimated a tentative orbital period of about 16 days.

The *H*- and K_s-band spectra are shown in Figs. 2 and 3 and the detected lines are reported in Table 5. The *H*-band spectrum is rather faint and exhibits very few lines. This is consistent

with a supergiant late O-type star (see e.g. Morel & Grosdidier 2005; Hanson et al. 1998). Moreover, the equivalent width of the He I absorption at 1.700 μm is closer to the value expected for a supergiant star than for a dwarf star (Hanson et al. 1998). The K_s-band spectrum shows Br(7–4) emission and a 2.1120 μm absorption lines with large equivalent widths that are compatible with those observed in O9.7 supergiant stars (see Hanson et al. 1996). Moreover, there are two other He I absorption lines at 2.0577 μm and 2.150 μm which lead to an ON9.7Iab stellar classification (Hanson et al. 1996).

3.8. IGR J16318-4848

IGR J16318-4848 is the first source discovered with INTEGRAL by the ISGRI detector on 20 January 2003 (Courvoisier et al. 2003). ToO observations, triggered with *XMM-Newton* provided a more accurate localization (Walter et al. 2003) and showed that the source was exhibiting a strong column density $N_{\rm H} \sim 2{\times}10^{24}$ cm^{-2} (Matt & Guainazzi 2003; Walter et al. 2003). Moreover, highly variable flux (by a factor of 20) with a time lapse of ten hours followed by two to three days of inactivity are signatures of wind accretion, reminiscent of other peculiar high energy sources such as XTE J0421+560/CI Cam and GX 301-2 (Revnivtsev et al. 2003). Using the *XMM-Newton* position, Filliatre & Chaty (2004) triggered ToO optical and NIR observations just after the detection of the source that led to the discovery of the counterpart, extremely bright in NIR and highly absorbed in the optical V-band (A_V = 17.4 mag). Nevertheless, this absorption in visible is 100 times lower than the absorption in X-rays. Thus, Filliatre & Chaty (2004) suggested that the material absorbing in the X-rays had to be concentrated around the compact object, while the material absorbing in optical/NIR would extend around the whole binary system. The NIR spectrum is very rich in many strong emission lines, originating from different media, that suggests the presence of a stratified circumstellar environment. This allowed Filliatre & Chaty (2004) to suggest the companion star to be a sgB[e], which are stars with extreme environments. Its position in the Hertzsprung-Russel diagram, at the edge of the blue supergiant domain, also confirms the extreme behavior of this object. Archival MIR data from *Spitzer* GLIMPSE survey showed a long wavelength ($\lambda \geqslant 4$ μm) excess. Fitting this excess with a blackbody model, Kaplan et al. (2006) concluded that it might be due to warm circumstellar dust emission. Subsequent *Spitzer*/IRS MIR spectroscopic observations, conducted by Moon et al. (2007) confirmed the hot ($T > 700$ K) circumstellar dust and also suggested a warm ($T \sim 190$ K) dust component. Rahoui et al. (2008), using MIR photometric observations with VLT/VISIR, built the optical to MIR SED and suggested a cocoon of dust that is enshrouding the whole binary system. With new VISIR MIR spectroscopic observations and using archival NTT + *Spitzer* observations, Chaty & Rahoui (2012) recently excluded the spherical geometry for the dust component and the warm dust component suggested by Moon et al. (2007) by fitting broadband NIR to MIR SED. Indeed, using an emission model of intermediate mass star such as Herbig Ae/Be stars adapted for sgB[e] stars, they showed the presence of two-temperature components in a toric geometry, with an irradiated toric rim of temperature $T_{\rm rim} \sim 3800$–5500 K, surrounded by a hot dusty viscous disk component at $T_{\rm dust} \sim 767$–923 K with a maximum extension of $r_{\rm out}$ = 5.6 AU.

We present our K_s-band spectrum in Fig. 3 and detected lines are reported in Table 5. It exhibits many intense and broad emission lines that were identified mainly according to Morris et al. (1996) and McGregor et al. (1988). Two lines (He I at 2.058 μm and He I at 2.1126 μm) show a P-Cygni profile, confirming that there is a strong stellar wind of circumstellar material. From these lines, we derived a wind speed value of $\sim$400 km s^{-1} consistent with the value previously derived by Filliatre & Chaty (2004). As underlined in Filliatre & Chaty (2004), many lines are common to CI Cam (Clark et al. 1999) indicating similar physical conditions. In contrast to the CI Cam and to the IGR J16318-4848 NIR spectra published by Filliatre & Chaty (2004), we detect in our K_s-band spectrum a line that could be an H_2 transition at 2.1218 μm, suggesting that either shock heating is high enough in this source or that there is a region of sufficiently low temperature where molecules such as H_2 are not dissociated (see Clark et al. 1999). Table 6 compares the equivalent width (EW) and FWHM values between data of 2003 (Filliatre & Chaty 2004) and data presented in this study, obtained in 2010. Assuming 20% of uncertainty for our EW and FWHM measurements (as noted above, and estimated after repeting the measurement process with the IRAF *splot* task), no major variation is detected for the brightest lines. Other lines such as [Fe II] at 2.046 μm, He I at 2.1126 μm, N III + C III at 2.116 μm, He I at 2.1847 μm, and [Fe II] at 2.224 μm, exhibit variations between 25 and 65%, but their faintness can engender more important uncertainties on EW and FWHM values, which prevents any further conclusion on these line variabilities.These observations confirm the sgB[e] nature of IGR J16318-4848.

3.9. IGR J16320-4751

IGR J16320-4751 was discovered in February 2003 by Tomsick et al. (2003) at the position RA = $16^{\rm h}32^{\rm m}.0$, Dec = –47°51′ (equinox J2000.0; uncertainty 2′.0). Follow-up *XMM-Newton* observations localized the source at RA = $16^{\rm h}32^{\rm m}01^{\rm s}.9$, Dec = –47°52′27″ (equinox J2000.0; uncertainty 3″) (Rodriguez et al. 2003, 2006). This result agrees with Negueruela & Schurch (2007). It is a heavily absorbed variable source with $N_{\rm H} \sim 2.1 \times 10^{23}$ cm^{-2} and a hard X-ray spectrum fitted by an absorbed power-law, with $\Gamma \sim 1.6$ (Rodriguez et al. 2006). Soft X-ray pulsations have been detected from this source at a period of $P \sim 1309 \pm 40$ s with *XMM-Newton* and $P \sim 1295 \pm 50$ s with ASCA; these pulsations are the signature of an X-ray pulsar (Lutovinov et al. 2005). An orbital period of 8.96 ± 0.01 days was found from a *Swift*/BAT lightcurve extending from 2004 December 21 to 2005 September 17 (Corbet & Remillard 2005), and of 8.99 ± 0.05 days with INTEGRAL (Walter et al. 2006). Plotting the spin and orbital periods of this source on a Corbet diagram Corbet et al. (2005) suggests a supergiant HMXB nature. IGR J16320-4751 might have been persistent for at least eight years, since this source is the rediscovery of a previously known ASCA source AX J1631.9-4752. NIR observations of the most likely counterpart, conducted by Chaty et al. (2008), showed that the blue NIR spectrum presents only an Fe line, probably because it is very faint and absorbed. The red NIR spectrum exhibits a very red continuum and the presence of absorption and emission lines: the Pa(7–3) emission line, the Brackett series with P-Cygni profiles between 1.5 and 2.17 μm and He I at 2.166 μm (perhaps with P-Cygni profile). According to Chaty et al. (2008), these narrow and deep Paschen and He I lines, associated with P-Cygni profiles, are typical of early-type stars, and more precisely of luminous supergiant OB stars, which is therefore the most likely spectral type of the companion star. The wide Brγ line would constrain the spectral type to an O supergiant or even O hypergiant. SED fitting computed in Rahoui et al. (2008) and observations of Chaty et al. (2008) finally state

that this source belongs to the very obscured supergiant HMXB class, hosting a neutron star.

In our K_s-band spectrum (see Fig. 4 and the detected lines in Table 5), the emission line of Br(7–4) is clearly detected at 2.1668 μm with possibly a P-Cygni profile. The He I emission line at 2.0586 μm is weak but quite broad, whereas another He I absorption line is detected at 2.1127 μm. These lines lead to a classification of the companion star as a BN0.5Ia according to Hanson et al. (2005), confirming the supergiant type of this HMXB. We point out that the spectrum exhibits numerous absorption lines that we were unable to associate with physical transitions, although we checked that these features do not come from a poor telluric correction.

3.10. IGR J16328-4726

IGR J16328-4726 was discovered with INTEGRAL by Bird et al. (2007). A flare, observed by Grupe et al. (2009), was detected with *Swift*/XRT on 2009 June 10 at the coordinates RA = $16^h32^m37\overset{s}{.}88$, Dec = –47°23′42″.4, (equinox J2000.0; uncertainty 1″.7). The XRT light curve shows that the source brightness is steadily decaying. Moreover, the X-ray spectrum in the XRT waveband can be fitted by an absorbed power law model with $\Gamma = 0.56^{+0.75}_{-0.68}$ and an absorption column density $N_H = 8.1^{+5.7}_{-4.9} \times 10^{22}$ cm^{-2} which tends to show an absorption excess in comparison with the expected galactic value. Because of this high absorption, Grupe et al. (2009) were unable to identify an optical counterpart. However, a 2MASS counterpart candidate is suggested at RA = $16^h32^m37\overset{s}{.}91$, Dec = –47°23′40″.9 (equinox J2000) with $J = 14.631$, $H = 12.423$, $K = 11.275$ mag. Corbet et al. (2010a) reported the analysis of the *Swift*/BAT 58-month survey light curve of the source in the energy range 15–100 keV that reveals highly significant modulation at a period near 10-days. The mean flux is approximatively of 1.3 mCrab. The 10 day period suggests that the source is an HMXB, in particular one powered by accretion from the wind of a supergiant companion star. According to Corbet et al. (2010a), this classification would be consistent with the high level of absorption found by Grupe et al. (2009). Fiocchi et al. (2010) used the INTEGRAL/IBIS-JEM-X public database and XRT observations performed during a flare of the source. Both spectral and timing properties observed during outburst, its Galactic plane location and the presence of an IR star in the *Swift*/XRT error circle suggest that this source is an SFXT. According to Fiocchi et al. (2010), the source 2MASS J16323791-4723409 is the most likely candidate IR counterpart. XMM-Newton observations, conducted by Bozzo et al. (2012), revealed a variability on timescales of hundreds of seconds, typical of SFXT prototypes. Finally, Fiocchi et al. (2013) identified the counterpart as a high-mass OB type star, classifying this source as a firm HMXB.

Our K_s-band spectrum (see Fig. 3 and Table 5) shows that the Br(7–4) emission line at 2.1661 μm is clearly detected. Moreover, He I at 2.0579 μm and at 2.1114 μm are detected in absorption, together with N III/C III emission around 2.116 μm. According to Hanson et al. (1996), it can be an O8Iaf or more probably an O8Iafpe, taking into account the He I/Br(7–4) line ratio and the N III/C III emission, which are typically observed in supergiant star spectra. Moreover, the C IV line also strengthens the supergiant classification of this system. This classification agrees with previous publications which suggested this source is an sgHMXB/SFXT.

3.11. IGR J16418-4532

IGR J16418-4532 was discovered in 2004 by Tomsick et al. (2004) with INTEGRAL at the position RA = 16^h41^m8, Dec = –45°32′ (equinox J2000.0; uncertainty 2′.0). *XMM-Newton* localized the source at RA = $16^h41^m51\overset{s}{.}0$, Dec = –45°32′25″ (equinox J2000.0; uncertainty 4″) (Walter et al. 2006). These observations have shown that it is a heavily absorbed X-ray pulsar exhibiting a column density of $N_H \sim 1.0 \times 10^{23}$ cm^{-2}, a peak-flux of ∼80 mCrab in the 20–30 keV band, and a pulse period of 1246 ± 100 s (Walter et al. 2006). Sguera et al. (2006), using INTEGRAL observations, suggested that this source is an SFXT candidate. A 3.75 day modulation was found in the *Rossi*-XTE/ASM and *Swift*/BAT lightcurves, with a possible total eclipse, which would suggest either a high binary inclination, or a supergiant companion star (Corbet et al. 2006). The latter case would be consistent with the position of the object in the Corbet diagram (Chaty et al. 2008). NIR observations conducted by Chaty et al. (2008) proposed four NIR candidate counterparts and the brightest one, 2MASS J16415078-4532253, is favored to be the candidate counterpart. SED fitting carried out by Chaty et al. (2008) suggested an OB spectral type companion star and the source would be a supergiant HMXB. But its X-ray behavior may rule out that this source belongs to the SFXT class. Rahoui et al. (2008) carried out SED fitting using NIR and MIR observations which gave an absorption in the V-band value of $A_V = 14.5$ even though the enshrouding material marginally contributes to its MIR emission. In February 2011, Romano et al. (2012) performed *Swift*/XRT observations confirming that the spectrum is well fitted by an absorbed power law. The source is quite bright, with maybe the signature of a flare characteristic of SFXT (see e.g. Romano et al. 2013). The 40 ks *XMM-Newton* observations carried out in February 2011 by Sidoli et al. (2012) show strong variability of two orders of magnitude with several bright flares. The type of X-ray variability displayed by IGR J16418-4532, its dynamic range and timescale, and the quasi-periodic flaring are all suggestive of a transitional accretion regime between pure wind accretion and full Roche lobe overflow according to Sidoli et al. (2012). Finally, Drave et al. (2013) used combined INTEGRAL and *XMM-Newton* observations to reveal an X-ray intensity dip in this pulsating SFXT, which may be explained by a highly magnetized neutron star.

The NIR K_s-band spectrum is presented in Fig. 3 and Table 5. It shows a wide emission line at 2.1672 μm that corresponds to the Br(7–4) line and a weak emission line of He I at 2.0580 μm. Moreover, we observed an absorption line of He I at 2.1124 μm. These detections point toward a BN0.5Ia spectral type[4] (see Fig. 6, right panel, for a comparison with the spectrum of IGR J16320-4751).

3.12. IGR J17200-3116

IGR J17200-3116 was discovered with INTEGRAL by **?**. *ROSAT* observations carried out by Stephen et al. (2005) refined the source coordinates and localized a possible USNO B1 counterpart with $B \sim 19$. The optical spectrum obtained by Masetti et al. (2006a) is typical of the HMXB class, clearly showing a narrow Hα line and a strongly reddened continuum. Moreover, Tomsick et al. (2008), using *Chandra* observations confirm the counterpart candidate suggested by Masetti et al. (2006a). The

[4] We point out that X-shooter observations (see Goldoni et al. 2013) show Br(7–4) line in absorption and then lead to an O9.5I spectral classification. Nevertheless, this result confirms the supergiant classification that we propose for this HMXB.

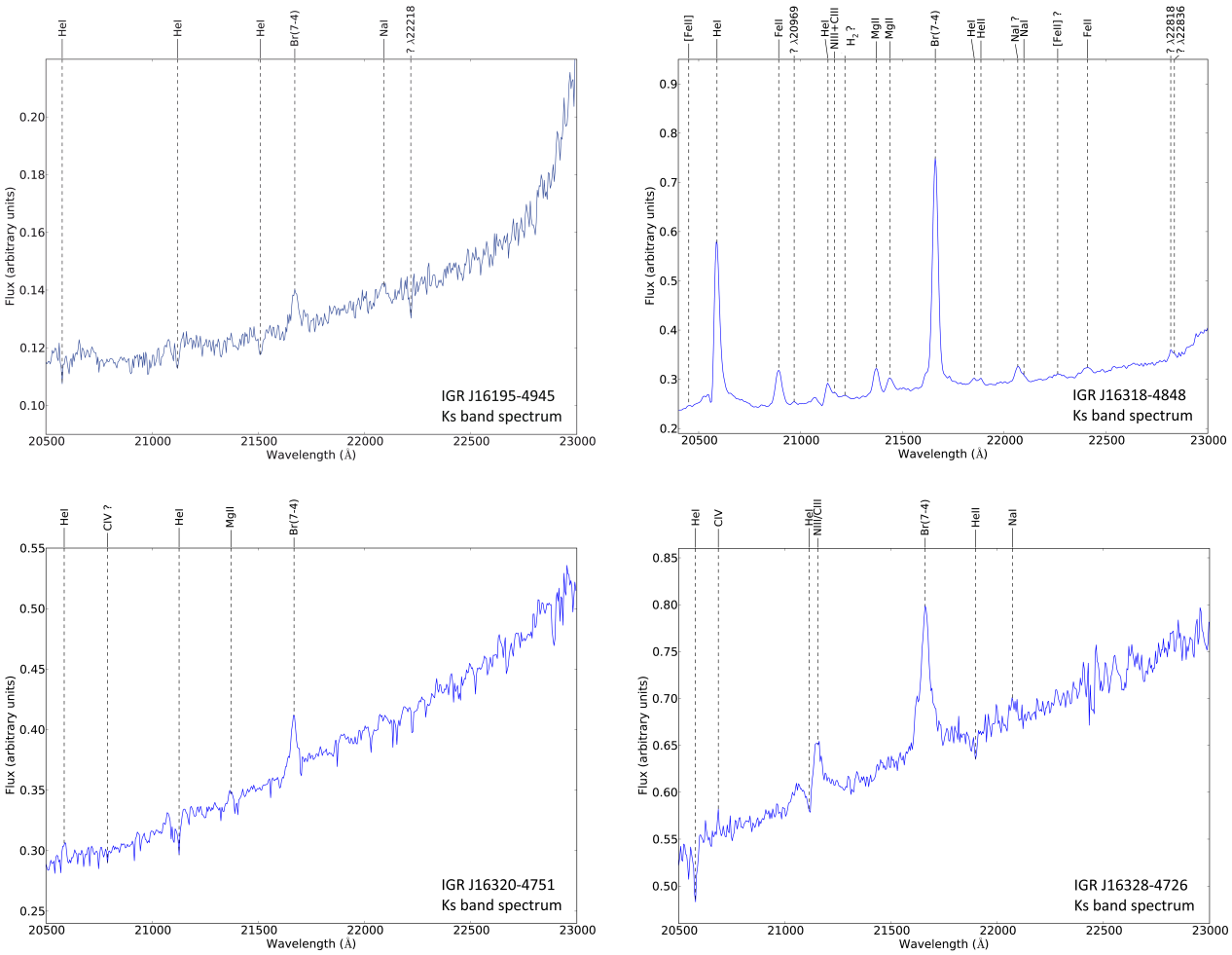


Fig. 3. Spectra of IGR J16195-4945 (*top left*, K_S-band), IGR J16318-4848 (*top right*), IGR J16320-4751 (*bottom left*), and IGR J16328-4726 (*bottom right*).

Chandra spectrum was fitted by an absorbed power law with $\Gamma = 0.8$ and $N_H = 1.9 \times 10^{23}$ cm^{-2}. This column density does not require local absorption. Finally, Nichelli et al. (2011), thanks to *Swift*/XRT X-ray light curves, detected coherent pulsations at a period of 328.182(3) s. This periodicity is confirmed in the 18–30 keV range by INTEGRAL/ISGRI archival observations from 2003 to 2006. All these results confirm the HMXB type of IGR J17200-3116.

The lack of optical photometry of this source prevents us from fitting the SED. In addition, due to bad weather, the NIR spectra are not useful. Thus, more observations are required to determine the spectral type of this HMXB.

3.13. IGR J17354-3255

IGR J17354-3255 was discovered with INTEGRAL by Bird et al. (2007). The *Swift* and *Chandra* observations carried out by Vercellone et al. (2009) and Tomsick et al. (2009) allowed the authors to locate the counterpart (2MASS J17352760-3255544) and show that the source is well fitted by an absorbed power law in the 0.3–10 keV range. Tomsick et al. (2009) suggest that the source is an HMXB. Moreover, D'Aì et al. (2011), using the *Swift*/BAT instrument, unveiled an 8.448 ± 0.002 days periodicity that is identified with the orbital period of the system, typical of a wind accretor X-ray binary. They also confirmed that the X-ray spectrum of the source is compatible with an HMXB X-ray spectral emission. Carrying out a long-term INTEGRAL monitoring of the source and using *Swift* archival observations, Sguera et al. (2011) showed that IGR J17354-3255 is a weak and persistent source that emits occasional X-ray flares. They also confirmed the orbital period of 8.4 days and claim that the spectral and temporal characteristics of the source are indicative of an sgHMXB, whereas the dynamic ranges at soft and hard X-rays tend to be typical of intermediate SFXT. Finally, Bozzo et al. (2012), using *XMM-Newton* spectra, claimed the source to be an SFXT.

The NIR K_s-band spectrum, presented in Fig. 4 and Table 5, shows a clear He I absorption at 2.1134 μm. A weak absorption is detected around 2.06 μm that could be an He I absorption. Thus, this spectrum points toward an O8.5Iab(f) (see Hanson et al. 1996) or an O9Iab (see Hanson et al. 2005) spectral type and confirms the sgHMXB/SFXT classification of the binary source.

3.14. IGR J17404-3655

IGR J17404-3655 was first mentioned by Bird et al. (2007). Landi et al. (2008), with a series of X-ray follow-up observations performed with *Swift*/XRT, determined an USNO and 2MASS counterpart. Moreover, Masetti et al. (2008), by carrying out spectroscopic observations, showed that the counterpart (USNO-A2.0.0525_28851523) presents a red continuum and a single narrow emission line consistent with the Hα line with an equivalent width of ∼17 Å. They concluded that the source is a

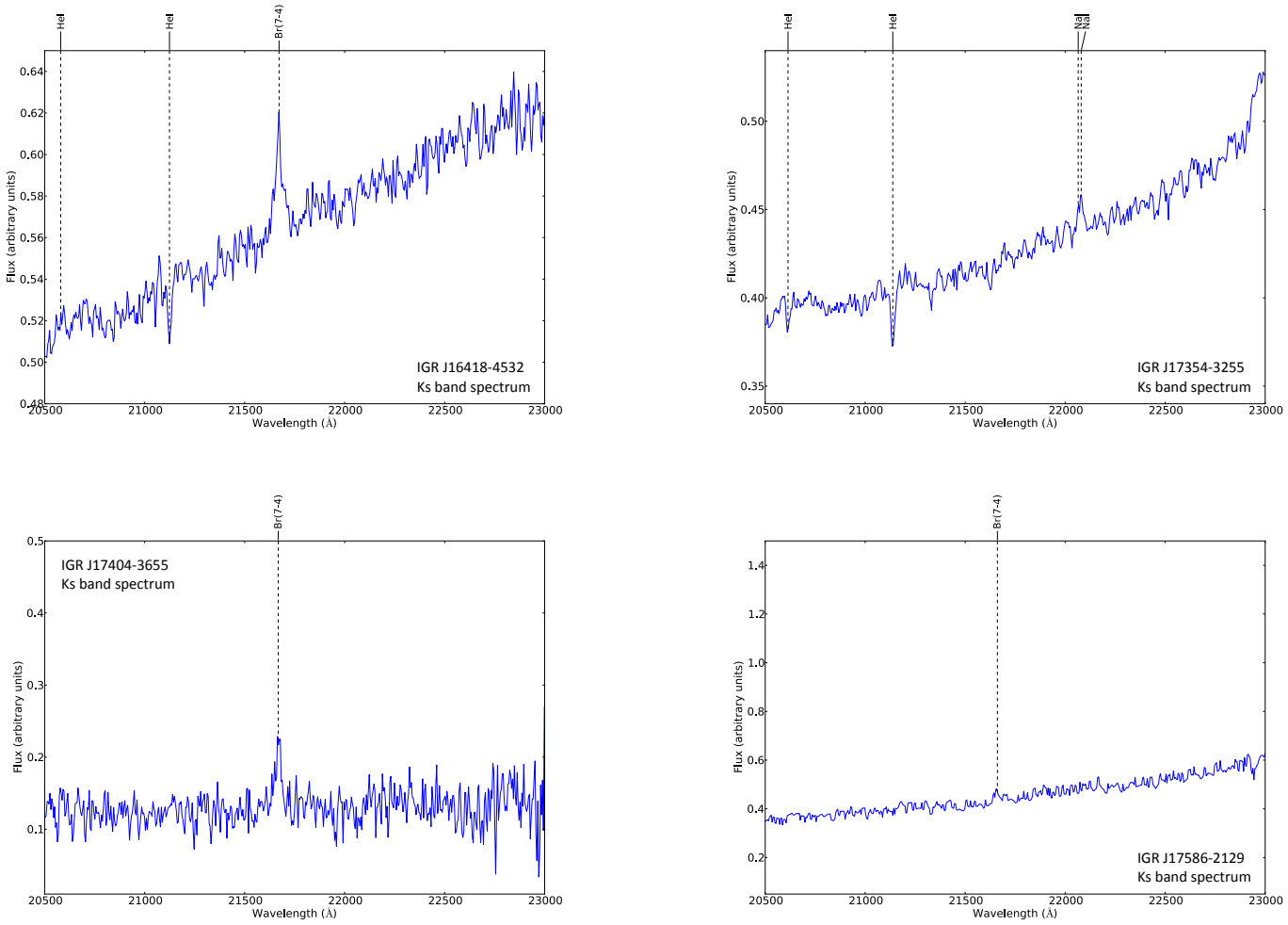


Fig. 4. Spectra of IGR J16418-4532 (*top left*), IGR J17354-3255 (*top right*), IGR J17404-3655 (*bottom left*), and IGR J17586-2129 (*bottom right*).

Galactic X-ray source, most likely a low-mass X-ray binary at a distance of 9.1 kpc (Masetti et al. 2009). Masetti et al. (2009) ruled out an HMXB nature for this source because the optical magnitudes do not fit any early spectral type. However, *Chandra* observations led by Tomsick et al. (2009) show that the spectrum is well fitted by an absorbed power law with a power-law index $\Gamma \sim -0.30^{+0.30}_{-0.24}$ which would be very unusual for an LMXB. Instead, these authors suggested that this source is an HMXB.

Only the Br(7–4) line is detected in emission in our NIR K_s-band spectrum (see Fig. 4 and Table 5). As for IGR J14331-6112 (see Sect. 3.5), assuming that the Brγ line is mainly detected in supergiant and Be stars (hardly ever in main-sequence stars), and knowing that in supergiant star spectra, He I at 2.058 μm in emission is generally detected as well, we argue that IGR J17404-3655 could be a Be star, since we do not detect any He I emission line at 2.058 μm. The low S/N prevents any firm classification, but if the source is an HMXB, it would probably be a BeHMXB. However, we cannot rule out the LMXB classification yet.

3.15. IGR J17586-2129

IGR J17586-2129 was discovered by Bird et al. (2007). Tomsick et al. (2009) localized the infrared 2MASS counterpart thanks to *Chandra* observations. The X-ray spectrum is well fitted by a power-law with $N_{\rm H} = 15.6 \times 10^{22}$ cm^{-2} and $\Gamma \sim 0.23$. The authors stated that the source is a candidate absorbed HMXB. *Swift* observations conducted by Krimm et al. (2009) during an outburst confirmed the association proposed by Tomsick et al. (2009). They fitted the data with a power-law with $N_{\rm H} = 1.11 \times 10^{23}$ cm^{-2} and $\Gamma \sim 1.14$. Finally, Sanchez-Fernandez et al. (2009), using INTEGRAL and *Swift*/BAT observations, derived an average flux over seven days of 11.2 mCrab in the 18–40 keV band. The 18–150 keV spectra were well fitted by a power-law with $\Gamma = 3.0$. Finally, if the spectrum remains unchanged, Sanchez-Fernandez et al. (2009) suggest that there is a cut-off in the 10–20 keV spectrum range.

Only the Br(7–4) line is detected in emission in our NIR K_s-band spectrum (see Fig. 4). Moreover, the SED (I, J, H, K_S, 3.4 μm, 4.6 μm, 12 μm, 22 μm photometry points) is well fitted (χ^2/d.o.f. = 5.0, see Fig. 5) with a model that combines two absorbed blackbodies: one representing the companion star emission, and another one representing a possible MIR excess due to absorbing material that enshrouds the companion star (see e.g. Rahoui et al. 2008). The free parameters of the fits are the absorption in V band, A_V, the radius to distance ratio R_*/D, the additional blackbody component temperature $T_{\rm d}$ and its radius $R_{\rm d}$. The stellar blackbody temperature was fixed to 20 000 K. The best-fitting parameters are stellar radius over distance $R_*/D = 5.47 \pm 0.27\ R_\odot$/kpc, along with a dust component: dust temperature $T_{\rm d} = 2033 \pm 304$ K, and spatial extension

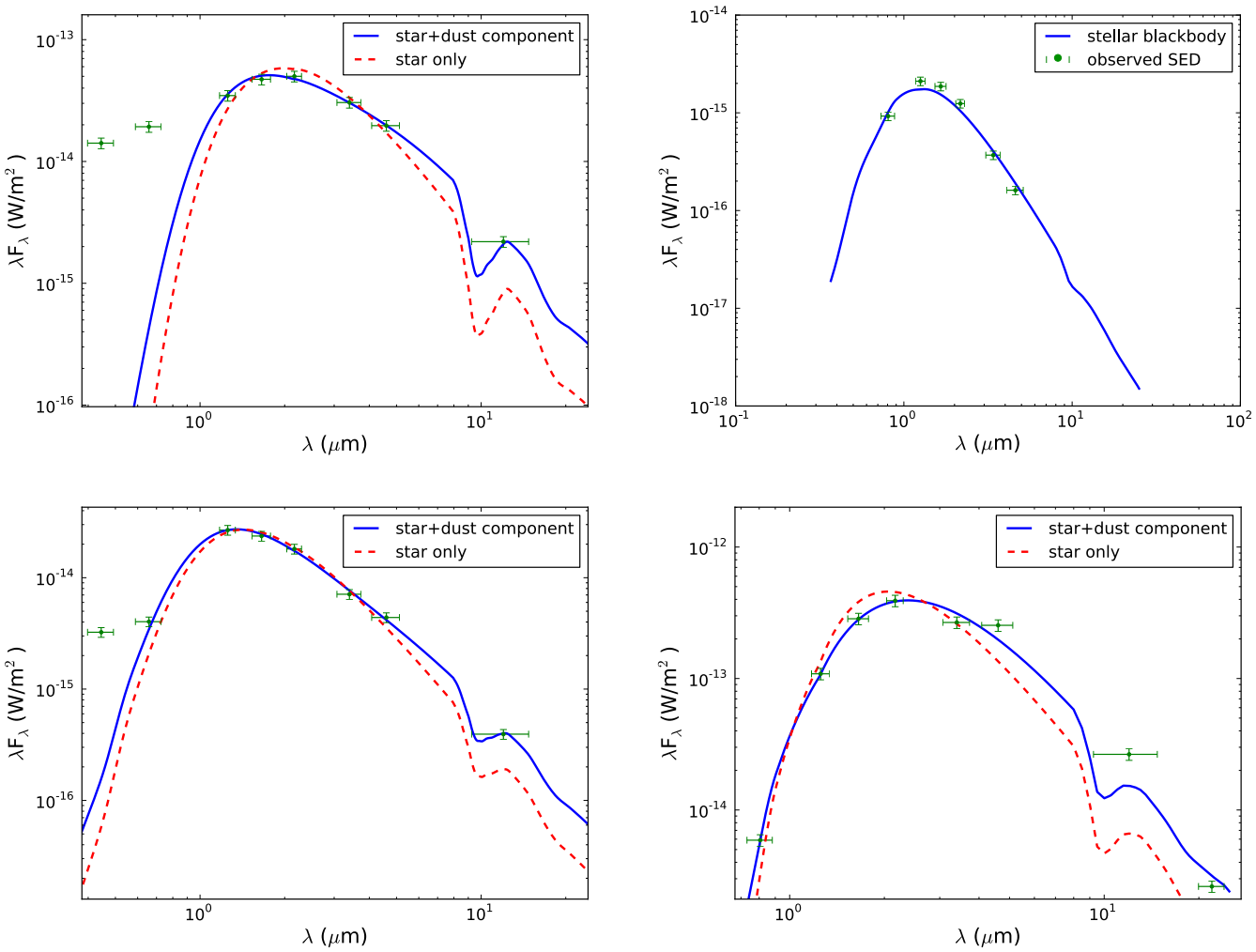


Fig. 5. Best fit of IGR J10101-5654 (*top left*), IGR J11187-5438 (*top right*), IGR 11435-6109 (*bottom left*), and IGR J17586-2129 (*bottom right*). Derived parameters are given in Table 7.

$R_{\rm d}/D = 49.01 \pm 7.35\ R_{\odot}$/kpc. The retrieved extinction value is equal to $A_V = 13.6 \pm 0.68$ mag. For comparison, the best-fitting parameters without the additional component are $A_V = 17.0 \pm 0.34$ mag; $R/D = 10.53 \pm 0.21\ R_{\odot}$/kpc, and χ^2/d.o.f. = 24.14. Thus, the SED fitting points toward a supergiant companion star.

3.16. Search for counterparts and study of the environment with WISE data

With the aim of studying the close environment of HMXB, we carried out a systematic search for counterparts in the WISE or GLIMPSE (when the source is blended) catalogs. This allows us to detect a MIR excess around the HMXB due to circumbinary dust (see the discussion for IGR J10101-5654, IGR J11435-6109, IGR J17586-2129), and examine the larger scale structures that probe the feedback of the source on its environment as well as the impact of the environment on the HMXB (see Fig. 7).

We present in Table 8 the fluxes in the four WISE filters for each detected source. Fluxes F_ν (in Jansky) were derived from the Vega magnitude $m_{\rm Vega}$, using the formula

$$F_\nu[\rm Jy] = F_{\nu 0} \times 10^{(-m_{\rm Vega}/2.5)}, \quad (1)$$

where $F_{\nu 0}$ is the zero-magnitude flux density derived for sources with power-law spectra $F_\nu \propto \nu^{-2}$ and listed in the WISE user manual[5] for each filter band. When the source was blended in the WISE data, we used the *Spitzer*/GLIMPSE data (see Table 9). GLIMPSE fluxes were directly imported from the GLIMPSE archive. We point out that IGR J14331-6112, and IGR J17404-3655 are not detected neither in WISE or GLIMPSE catalogs whereas IGR J14488-5942 and IGR J17354-3255 are blended both in the GLIMPSE and WISE catalogs.

Most of the sources studied here were detected at 3.4 μm and 4.6 μm (see Table 8) or at 3.6 and 4.5 μm (when *Spitzer*/IRAC data were used instead). Two sources (IGR J16318-4848 and IGR J17586-2129) were detected even at 22 μm which can be explained by a substantial quantity of circumstellar dust, consistent with previous observations of these two sources (see Sects. 3.8 and 3.15).

We also examined the close environment of the sources and searched for cavity-shaped-structures around the sources that might trace an interaction with the close environment. We only detected a cloud with a cavity surrounding IGR J11435-6109 (see Fig. 7). This structure may be associated with the HMXB. A more detailed and comprehensive investigation of this aspect will be the topic of a forthcoming paper.

[5] Available at this address: `http://WISE2.ipac.caltech.edu`

Table 5. Spectroscopy results for all the sources.

Source	Line	λ (μm)	$\lambda_{\rm fit}$ (μm)	Flux (arbitrary units)	EW (Å)	$FWHM$ (Å)
IGR J10101-5654						
			H band			
	Br(20–4)	1.519	1.5198	455.8	–1.383	19.87
	Br(19–4)	1.525	1.5265	93.22	–0.279	4.304
	Br(18–4)	1.534	1.5354	555.4	–1.662	23.57
	Br(17–4)	1.543	1.5451	634.1	–1.905	24.53
	Br(16–4)	1.555	1.5568	901.8	–2.692	24.88
	Br(15–4)	1.569	1.5708	707.6	–2.031	25.34
	N III + C III	1.575	1.5778	841.4	–2.439	44.81
	+ Fe II	1.576				
	Br(14–4)	1.588	1.5901	1481	–4.134	32.46
	Br(13–4)	1.611	1.6120	1151	–3.167	31.88
	Br(12–4)	1.641	1.6410	634.9	–1.649	15.93
	[Fe II]	1.643	1.6427	572	–1.488	12.58
	Br(11–4)	1.681	1.6822	1121	–2.645	25.33
	Fe II	1.688	1.6893	154.5	–0.363	7.551
	[Fe II]	1.711	1.7122	362.5	–0.824	15.66
	Br(10–4)	1.736	1.7377	1032	–2.062	24.4
			$K_{\rm s}$ band			
	He I	2.058	2.0586	1537	–4.47	57.47
	H_2	2.1218	2.1226	269.1	–0.491	10.59
	Mg II	2.138	2.1363	326.9	–0.901	35.5
	Mg II	2.144	2.1454	344.9	–0.941	24.12
	Br(7–4)	2.166	2.1659	2249	–5.952	29.98
	He II	2.1891	2.1886	334.1	–0.872	20.2
	Na I	2.206	2.2064	328.2	–0.833	15.24
IGR J11435-6109						
			H band			
	Br(21–4)	1.513	1.5137	310.8	–1.285	24.42
	Br(20–4)	1.519	1.5200	316.3	–1.323	23.2
	Br(19–4)	1.525	1.5260	512.6	–2.178	31.92
	Br(18–4)	1.534	1.5349	652.3	–2.799	26.48
	Br(17–4)	1.543	1.5441	571.6	–2.458	28.05
	Br(16–4)	1.555	1.5568	472.2	–1.993	28.01
	Br(15–4)	1.569	1.5707	528.9	–2.205	24.76
	N III + C III	1.575	1.5772	344.1	–1.43	22.46
	+ Fe II	1.576				
	Br(14–4)	1.588	1.5895	1013	–4.158	31.53
	Br(13–4)	1.611	1.6119	957.2	–3.896	43.94
	Br(12–4)	1.641	1.6414	894.7	–3.508	38.21
	Br(11–4)	1.681	1.6813	1032	–3.8	36.15
	He I	1.700	1.7014	53.19	–0.19	4.389
	[Fe II] ?	1.711	1.7120	306.2	–1.101	20.43
	Br(10–4)	1.736	1.7364	973.4	–3.225	27.62
			$K_{\rm s}$ band			
	He I	2.058	2.0590	384.9	–2.788	33.86
	Mg II	2.138	2.1385	193.8	–1.367	33.36
	Mg II	2.144	2.1444	91.25	–0.637	8.416
	Br(7–4)	2.166	2.1664	273.9	–1.805	16.35
	He II	2.1891	2.1893	125.7	–0.83	20.09
IGR J13020-6359						
			$K_{\rm s}$ band			
	He I	2.058	2.0594	714.3	–2.734	25.74
	Br(7–4)	2.166	2.1663	2962	–9.986	29.09
IGR J14331-6112						
			$K_{\rm s}$ band			
	Br(7–4)	2.166	2.1657	184.3	–4.148	34.54
IGR J14488-5942						
			$K_{\rm s}$ band			
	He I	2.058	2.0590	446.6	–9.32	39.86
	Br(7–4)	2.166	2.1665	357.5	–5.722	35.7
IGR J16195-4945						
			H band			
	Br(19–4)	1.525	1.5251	113.2	–1.134	7.221
	Br(18–4)	1.534	1.5339	177.4	–1.808	11.44
	Br(16–4)	1.555	1.5566	137.5	–1.422	10.83
	[Fe II] ?	1.599	1.5975	337.4	–3.148	16.79
	Br(13–4)	1.611	1.6129	213.4	–1.852	14.22
	He I	1.700	1.6998	–731.6	3.87	41.00

Table 6. Equivalent width and FWHM values of IGR J16318-4848.

Line	λ (μm)	EW (Å) – 2010 data	EW (Å) – 2003 data	$FWHM$ (Å) – 2010 data	$FWHM$ (Å) – 2003 data
[Fe II]	2.046	–0.427	–1	20.54	26
He I	2.058	–38.38	–42	29.34	35
Fe II	2.089	–10.89	–13	36.01	36
He I	2.1126	–3.756	–5	25.47	43
N III + C III	2.116	–1.813	–4 (?)	30.62	44 (?)
Mg II	2.138	–6.139	–8	30.58	35
Br(7–4)	2.1661	–52.55	–45	32.28	36
He I	2.1847	–1.411	–7 (?)	30.17	50
Na I ?	2.2056	–3.526	–3	31.06	40
Na I	2.209	–1.337	blended	30.35	blended
[Fe II]	2.224	–1.974	–0	64.4	21
Fe II	2.240	–1.827	–2	41.35	40

Notes. Comparison of our data with those of Filliatre & Chaty (2004). No major variation are detected for the brightest lines. Other lines exhibit variations between 25% and 65%, but their faintness prevents any further conclusion on their variabilities.

Table 7. Parameters derived from SED fitting.

Source	A_V (mag)	T_* (K)	R/D ($R_\odot$/kpc)	T_d (K)	R_d/D ($R_\odot$/kpc)	χ^2/d.o.f.	d.o.f.
IGR J10101-5654	13.1 ± 0.86	20 000	2.79 ± 0.20	1016 ± 127	28.3 ± 4.25	2.23	2
IGR J11187-5438	3.9 ± 0.40	6000	0.60 ± 0.03	–	–	3.45	3
IGR J11435-6109	7.98 ± 0.44	20 000	1.33 ± 0.050	925.6 ± 190.7	51.6 ± 2.97	1.14	2
IGR J17586-2129	13.6 ± 0.68	20 000	5.47 ± 0.27	2033 ± 3045	49.01 ± 7.35	5.0	4

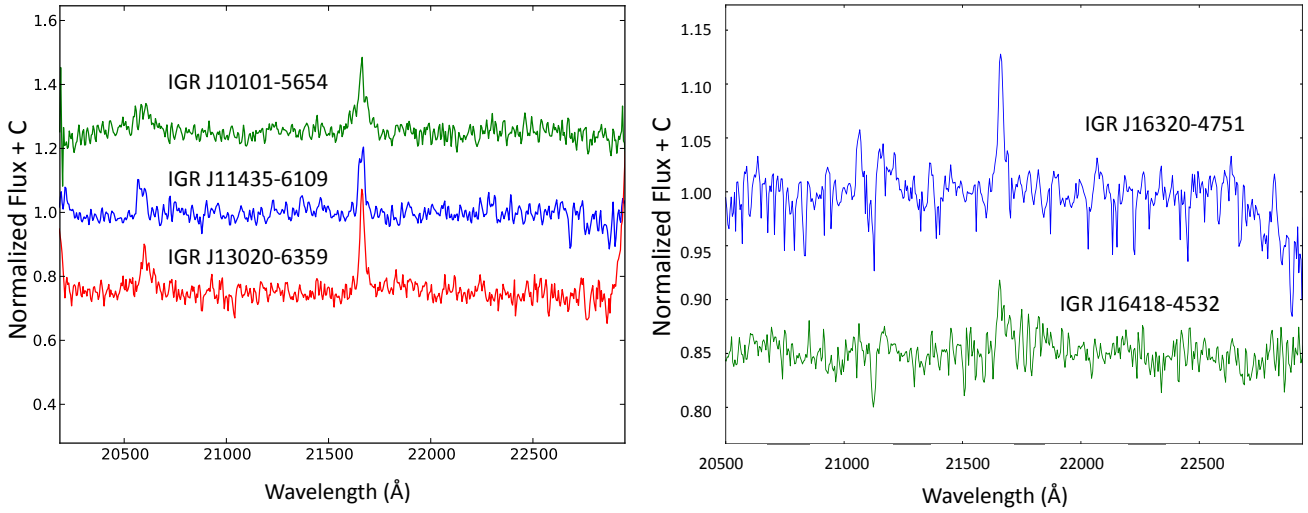


Fig. 6. *Left panel*: comparison of the K_s-band spectra of IGR J10101-5654, IGR J11435-6109, and IGR J13020-6359 (spectra are normalized and offset). *Right panel*: comparison of the K_s-band spectra of IGR J16320-4751, and IGR J16418-4532 (spectra are normalized and offset).

Table 8. WISE counterpart magnitudes.

Source name	3.4 μm flux (mJy)	4.6 μm flux (mJy)	12 μm flux (mJy)	22 μm flux (mJy)
IGR J10101-5654	36.07 ± 0.764	29.14 ± 0.564	8.788 ± 0.364	<5.227
IGR J11187-5438	0.437 ± 0.024	0.239 ± 0.018	<0.877	<5.227
IGR J11435-6109	8.416 ± 0.217	6.506 ± 0.174	1.576 ± 0.128	<5.227
IGR J16195-4945	23.07 ± 0.638	17.19 ± 0.490	<0.877	<5.227
IGR J16318-4848	1001 ± 47	1135 ± 25	310 ± 5.4	297 ± 7.7
IGR J17586-2129	316 ± 9.3	376 ± 7.3	116 ± 1.8	46.97 ± 2.163

Table 9. *Spitzer*/GLIMPSE counterpart magnitudes for the blended or undetected sources in the WISE point source catalog.

Source name	3.6 μm flux (mJy)	4.5 μm flux (mJy)	5.8 μm flux (mJy)	8.0 μm flux (mJy)
IGR J13020-6359	11.57 ± 0.673	9.157 ± 1.025	7.269 ± 0.559	4.690 ± 0.455
IGR J16320-4751	42.04 ± 1.814	42.89 ± 2.010	36.20 ± 1.553	17.76 ± 0.951
IGR J16328-4726	23.14 ± 1.052	21.40 ± 1.140	16.22 ± 0.754	10.01 ± 0.405
IGR J16418-4532	11.81 ± 0.642	9.352 ± 0.566	5.855 ± 0.463	3.394 ± 0.218

4. Discussion

In this section we discuss the number of BeHMXB versus the number of sgHMXB currently identified and the implications of this ratio. We focus only on the HMXB for which a spectral type has been derived.

Of the 114 HMXB candidates listed in the Liu catalog of HMXB (Liu et al. 2006), 39 are confirmed as BeHMXB and 18 as sgHMXB (see Liu et al. 2006). We therefore considered all INTEGRAL source HMXB candidates contained in the Liu catalog and not confirmed yet. For these objects, we retrieved the identification (when available) in the INTEGRAL source catalog maintained by J. Rodriguez and A. Bodaghee[6]. We added to these sources all the other INTEGRAL sources identified since 2006 and the 13 sources identified in the present article (see Table 10). This left us with 44 confirmed BeHMXB and 37 confirmed sgHMXB. Six sources are mentioned to have peculiar features in the Liu catalog: CI Cam, IGR J16318-4848, Cyg X-3, LS 5039, V4641 Sgr, and SS 433. We add two objects to this list: IGR J10101-5654 and IGR J19113+1533 which seem to show the B[e] phenomenon (see Sect. 3.1 for IGR J10101-5654 and Masetti et al. 2010 for IGR J19113+1533).

Before INTEGRAL, there were 42% confirmed BeHMXB and only 4% confirmed sgHMXB out of the total number of HMXB catalogd in Liu et al. (2000). The INTEGRAL observations have led to the discovery of a significant number of sgHMXB, causing a dramatic increase in the fraction of HMXB that are sgHMXB. Indeed, based on this study, we reach the following statistics for the HMXB confirmed by spectral type: 49% BeHMXB, 42% sgHMXB and 9% peculiar HMXB (see Fig. 8).

The majority of sgHMXB currently discovered suffers from huge X-ray absorption that explains why these sources were not detected before the INTEGRAL launch. Because of this substantial absorption they were not detected in the soft X-ray domain, which was well covered by the previous high-energy instruments. By observing the sky beyond 10 keV, where the photoelectric absorption becomes negligible, INTEGRAL enabled to discover these obscured sources, making their population rapidly growing over the last ten years. Moreover, the high sensitivity of the INTEGRAL detectors, which enables one to discover sources with a very low quiescent level ($\sim 10^{33}$ erg s^{-1}), and their large field of view also facilitated detecting new obscured sgHMXB.

Finally, the number of HMXB discovered with INTEGRAL and identified thanks to infrared observations is now high enough to carry out a population study of this family of high-energy sources and to accurately study their formation and evolution.

We now would like to place these source-type statistics into the context of HXMB evolution. HMXB are divided into two classes: sgHMXB and BeHMXB. In both classes, the X-ray source is generally a neutron star powered by accretion of matter coming from the companion star. Accretion in sgHMXB can be driven by Roche lobe overflow or a stellar wind, whereas in BeHMXB, the companion star is not filling its Roche-lobe and the neutron star generally accretes matter when passing through the decretion disk located around the companion. Formation of BeHMXB and sgHMXB is explained by two different scenarii, principally controlled by physical parameters such as the transfer of mass and angular momentum, the spin and metallicity of the stars, or the kick experienced during the supernova event. BeHMXB are formed following the rejuvenation model of Rappaport et al. (1982), in which the mass transfer engenders the formation of a decretion disk around the companion star. These systems, showing wide orbital eccentricities, are the result of massive binaries that undergo a semi-conservative mass transfer evolution. On the other hand, sgHMXB evolution is driven by the common-envelope phenomenon, during which the compact object enters inside the envelope of the companion star. Thus, its orbital period is rapidly decreasing via a significant loss of orbital angular momentum (see e.g. Chaty 2011).

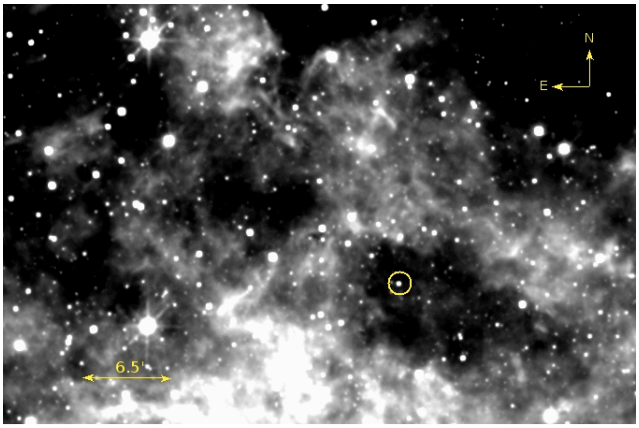


Fig. 7. WISE 12 μm image of the region around IGR J11435-6109.

INTEGRAL observations have raised new questions about HMXB evolution, particularly by discovering two new classes of sgHMXB that were previously undetected. The first one is composed of very obscured sgHMXB, exhibiting huge local extinction, and the others are sgHMXB showing fast and transient outbursts, called SFXTs (Negueruela et al. 2006, 2008). Obscured HMXB are exhibiting complex and stratified circumstellar material. Some of these sgHMXB present the B[e] phenomenon (such as IGR J10101-5654 or IGR J16318-4848, see Sects. 3.8 and 3.1). Lamers et al. (1998) defined these sources as stars that i. emit forbidden lines of [Fe II] and [O I]; ii. exhibit a strong MIR excess due to hot circumstellar dust; iii. present P-Cygni line profiles, which are characteristic of huge mass-loss. The peculiarities of these objects may be explained by ejections of matter during phases of interaction with the compact object (see e.g. Kraus et al. 2010; Wheelwright et al. 2012). Indeed, according to Wheelwright et al. (2012), at least 50% of the sgB[e] stars observed at high spatial resolution may be interacting binaries, which raises the possibility that binarity plays an important role in this process. Observing these obscured sgB[e] HMXB sources, which seem to be composed of a dusty disk (see e.g.

[6] http://irfu.cea.fr/Sap/IGR-Sources

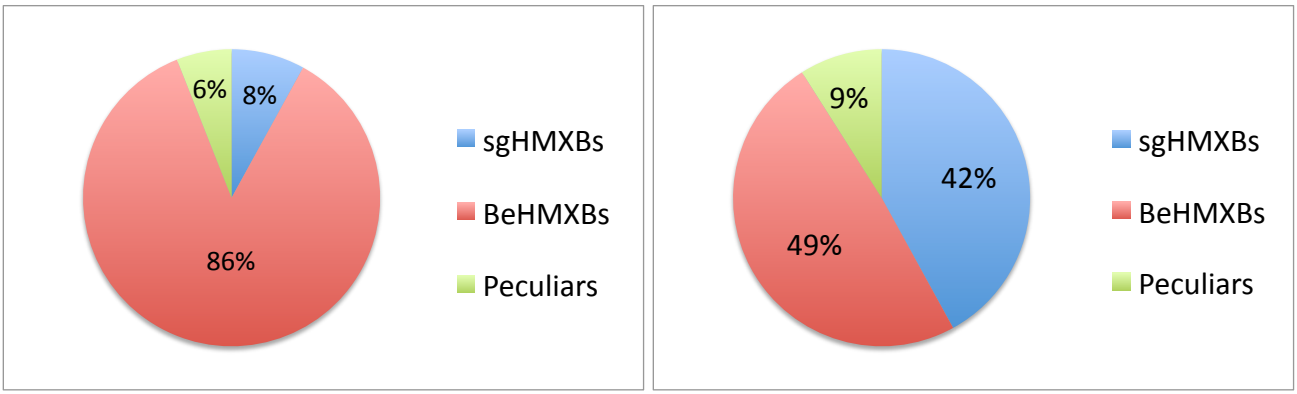


Fig. 8. *Left panel*: fraction (in percents) of confirmed (with spectral type) sgHMXB, BeHMXB and peculiar HMXB (such as B[e]HMXB) in Liu et al. (2000) catalog. *Right panel*: fraction (in percents) of confirmed (with spectral type) sgHMXB, BeHMXB and peculiar HMXB (such as B[e]HMXB) to date.

Table 10. Summary of results on HMXB spectral type (SpT) presented in this study.

Source	NIR Counterpart RA (J2000)	NIR Counterpart Dec (J2000)	Previous identification	Derived SpT (this pap
IGR J10101-5654	10:10:11.87	–56:55:32.1	HMXB ? (1,2)	sgB[e]
IGR J11187-5438	11:18:21.21	–54:37:28.6	?	LMXB ?
IGR J11435-6109	11:44:00.30	–61:07:36.5	B2III or B0V (3)	B0.5Ve
IGR J13020-6359	13:01:58.7	–63:58:09.0	Be (4)	B0.5Ve
IGR J14331-6112	14:33:08.33	–61:15:39.7	BIII or BV, Be ? (5)	Be ?
IGR J14488-5942	14:48:43.33	–59:42:16.3	Be ? (6)	Oe/Be
IGR J16195-4945	16:19:32.20	–49:44:30.5	O/B supergiant (7)	ON9.7Iab
IGR J16318-4848	16:31:48.31	–48:49:00.7	sgB[e] (8)	sgB[e]
IGR J16320-4751	16:32:01.75	–47:52:28.9	O supergiant ? (9,10)	BN0.5Ia
IGR J16328-4726	16:32:37.91	–47:23:40.9	O/B supergiant ? (11)	O8Iafpe
IGR J16418- 4532	16:41:50.79	–45:32:25.3	O/B supergiant (12)	BN0.5Ia
IGR J17200-3116	17:20:06.1	–31:17:02.0	HMXB ? (2)	?
IGR J17354-3255	17:35:27.60	–32:55:54.40	sgHMXB ? (13)	O9Iab
IGR J17404-3655	17:40:26.85	–36:55:37.6	LMXB ? / HMXB ? (3,14)	Be ?
IGR J17586-2129	17:58:34.56	–21:23:21.53	HMXB ? (14)	supergiant O/B

Reference. (1) Tomsick et al. (2008); (2) Masetti et al. (2006a); (3) Masetti et al. (2009); (4) Chernyakova et al. (2005); (5) Masetti et al. (2008); (6) Corbet et al. (2010a); (7) Tomsick et al. (2006); (8) Filliatre & Chaty (2004); (9) Corbet et al. (2005); (10) Chaty et al. (2008); (11) Fiocchi et al. (2013); (12) Sguera et al. (2006); (13) Sguera et al. (2011); (14) Tomsick et al. (2009).

Chaty & Rahoui 2012 and Servillat et al., in prep.), is a step forward in the understanding of circumstellar environment of evolved massive stars. Other sgB[e], at a different evolutionary stage, also exhibit a disk probably formed after an efficient mass-transfer (see e.g. Millour et al. 2011) and the link with these objects should be investigated.

All these results about sgHMXBs can be combined to explain the observed differences by different orbital configurations (see e.g. Chaty 2011): obscured sgHMXB are composed of a neutron star orbiting a supergiant star at a few stellar radii that emits persistent X-ray emission, whereas in SFXTs, a neutron star is orbiting the supergiant in a large and eccentric orbit, accreting clumps of matter when it comes close to the companion star. This scenario describes the properties currently observed in HMXB quite well, even though some questions still remain open. For example, no purely wind accreting sgHMXB with a black hole has been detected yet (Cygnus X-1 is accreting both wind and disk matter), probably because massive stars lose too much mass to finish their life as a black hole. Likewise, the rarity of HMXB that host a companion Wolf-Rayet star (only Cygnus X-3 is known) was underlined over the years and places constraints on evolution of HMXB (see Linden et al. 2012; Lommen et al. 2005). Lommen et al. (2005) also suggested that several X-ray binaries with core helium-burning companions should be observed in the Milky Way. They are expected to exhibit high intrinsic absorption mainly due to X-ray absorption by stellar wind. Companion stars of these obscured sgHMXB could evolve as follows (Kogure & Leung 2007): O → Of → WN (hydrogen-rich) → LBV → WN (hydrogen-poor) → WC → SN: starting their life as an O star on the main-sequence, then evolving as an LBV star, and finally finishing their life as a Wolf-Rayet star. sgB[e] and LBV companions are probably at the interface between hydrogen- and helium-burning core and could then partly explain the expected population described by Lommen et al. (2005).

Finally, studying HMXB is of interest for a wide range of astrophysics subjects. Indeed, it has been shown by Mirabel et al. (2011) that black hole HMXB could have determined the early thermal history of the Universe and contributed to its reionization, between 380 000 and 1 billion years after the Big Bang. Moreover, HMXB act as a good tracer of recent star formation in galaxies because of their short lives (see e.g. Mineo et al. 2011; Bodaghee et al. 2012; Coleiro & Chaty 2013). It has been shown by Sana et al. (2012) that almost three quarters of the very bright high-mass stars do not live alone, most of them experience interactions such as mass transfer during their life, which makes

them an interesting bridge between HMXB and stellar evolution investigations.

5. Conclusion

We have presented results of a large NIR observing campaign carried out in 2008 and 2010 using ESO/NTT facilities. These photometric and spectroscopic data allowed us to constrain and/or confirm the spectral type of 13 HMXB in the Milky Way reported in Table 10. The proportion of confirmed sgHMXB is now 42%, 49% are confirmed BeHMXB, and 9% are peculiar sources. Moreover, we conducted a systematic search of MIR counterparts in the WISE data release to detect any MIR excess due to hypothetical circumstellar dust, but also with the aim of examining the larger-scale environment that presents possible interaction and feedback. Finally, we recommend additional investigations of the three sources that have a MIR excess (IGR J10101-5654, IGR J11435-6109, and IGR J17586-2129) to assess the physical conditions in their close environment.

Acknowledgements. We warmly thank the anonymous referee for constructive comme,ts that allowed us to improve the manuscript.This work was supported by the Centre National d'Études Spatiales (CNES), based on observations obtained with MINE – the Multi-wavelength INTEGRAL NEtwork–. JAT acknowledges partial support from NASA through *Chandra* Award Number GO1-12046X issued by the *Chandra* X-ray Observatory Center, which is operated by the Smithsonian Astrophysical Observatory under NASA contract NAS8-03060. This research has made use of the IGR Sources page maintained by J. Rodriguez & A. Bodaghee (`http://irfu.cea.fr/Sap/IGR-Sources`); of data products from the Two Micron All Sky Survey, which is a joint project of the University of Massachusetts and the Infrared Processing and Analysis Center/California Institute of Technology, funded by the National Aeronautics and Space Administration and the National Science Foundation; of the SIMBAD database and the VizieR catalog access tool, operated at CDS, Strasbourg, France; of NASA's Astrophysics Data System Bibliographic Services as well as of the NASA/IPAC Infrared Science Archive, which is operated by the Jet Propulsion Laboratory, California Institute of Technology, under contract with the National Aeronautics and Space Administration.

References

Bird, A. J., Barlow, E. J., Bassani, L., et al. 2006, ApJ, 636, 765
Bird, A. J., Malizia, A., Bazzano, A., et al. 2007, ApJS, 170, 175
Bird, A. J., Bazzano, A., Bassani, L., et al. 2010, ApJS, 186, 1
Bodaghee, A., Tomsick, J. A., Rodriguez, J., & James, J. B. 2012, ApJ, 744, 108
Bozzo, E., Pavan, L., Ferrigno, C., et al. 2012, A&A, 544, A118
Chaty, S. 2011, in Evolution of Compact Binaries, eds. L. Schmidtobreick, M. R. Schreiber, & C. Tappert, ASP Conf. Ser., 447, 29
Chaty, S., & Rahoui, F. 2012, ApJ, 751, 150
Chaty, S., Rahoui, F., Foellmi, C., et al. 2008, A&A, 484, 783
Chen, H., Bally, J., O'dell, C. R., et al. 1998, ApJ, 492, L173
Chernyakova, M., Lutovinov, A., Rodríguez, J., & Revnivtsev, M. 2005, MNRAS, 364, 455
Clark, J. S., Steele, I. A., Fender, R. P., & Coe, M. J. 1999, A&A, 348, 888
Coleiro, A., & Chaty, S. 2013, ApJ, 764, 185
Corbet, R. H. D., & Remillard, R. 2005, ATel, 377, 1
Corbet, R., Barbier, L., Barthelmy, S., et al. 2005, ATel, 649, 1
Corbet, R., Barbier, L., Barthelmy, S., et al. 2006, ATel, 779, 1
Corbet, R. H. D., Barthelmy, S. D., Baumgartner, W. H., et al. 2010a, ATel, 2588, 1
Corbet, R. H. D., Barthelmy, S. D., Baumgartner, W. H., et al. 2010b, ATel, 2598, 1
Courvoisier, T. J.-L., Walter, R., Rodriguez, J., Bouchet, L., & Lutovinov, A. A. 2003, IAU Circ., 8063, 3
D'Aì, A., La Parola, V., Cusumano, G., et al. 2011, A&A, 529, A30
Drave, S. P., Bird, A. J., Sidoli, L., et al. 2013, MNRAS, 433, 528
Filliatre, P., & Chaty, S. 2004, ApJ, 616, 469
Fiocchi, M., Sguera, V., Bazzano, A., et al. 2010, ApJ, 725, L68
Fiocchi, M., Bazzano, A., Bird, A. J., et al. 2013, ApJ, 762, 19
Goldoni, P., Chaty, S., Goldwurm, A., & Coleiro, A. 2013 [arXiv:1302.0714]
Grebenev, S. A., Ubertini, P., Chenevez, J., et al. 2004, ATel, 350, 1
Grupe, D., Kennea, J., Evans, P., et al. 2009, ATel, 2075, 1
Hanson, M. M., Conti, P. S., & Rieke, M. J. 1996, ApJS, 107, 281
Hanson, M. M., Rieke, G. H., & Luhman, K. L. 1998, AJ, 116, 1915
Hanson, M. M., Förster Schreiber, N. M., Cresci, G., et al. 2005, ApJS, 161, 154
in't Zand, J., & Heise, J. 2004, ATel, 362, 1
Kaplan, D. L., Moon, D.-S., & Reach, W. T. 2006, ApJ, 649, L107
Keek, S., Kuiper, L., & Hermsen, W. 2006, ATel, 810, 1
Kogure, T., & Leung, K.-C. 2007, The Astrophysics of Emission-Line Stars, Astrophys. Space Sci. Lib., 342
Kraus, M., Borges Fernandes, M., & Chesneau, O. 2010, in Binaries – Key to Comprehension of the Universe, eds. A. Prša, & M. Zejda, ASP Conf. Ser., 435, 395
Krimm, H. A., Kennea, J. A., Barthelmy, S. D., et al. 2009, ATel, 2156, 1
Kuiper, L., Keek, S., Hermsen, W., Jonker, P. G., & Steeghs, D. 2006, ATel, 684, 1
Lamers, H. J. G. L. M., Zickgraf, F.-J., de Winter, D., Houziaux, L., & Zorec, J. 1998, A&A, 340, 117
Landi, R., Masetti, N., Bassani, L., et al. 2007, ATel, 1273, 1
Landi, R., Masetti, N., Malizia, A., et al. 2008, ATel, 1539, 1
Landi, R., Masetti, N., Capitanio, F., Fiocchi, M., & Bird, A. J. 2009, ATel, 2355, 1

Linden, T., Valsecchi, F., & Kalogera, V. 2012, ApJ, 748, 114
Liu, Q. Z., van Paradijs, J., & van den Heuvel, E. P. J. 2000, A&AS, 147, 25
Liu, Q. Z., van Paradijs, J., & van den Heuvel, E. P. J. 2006, A&A, 455, 1165
Lommen, D., Yungelson, L., van den Heuvel, E., Nelemans, G., & Portegies Zwart, S. 2005, A&A, 443, 231
Lutovinov, A., Rodriguez, J., Revnivtsev, M., & Shtykovskiy, P. 2005, A&A, 433, L41
Lutovinov, A. A., Revnivtsev, M. G., & Tsygankov, S. S., & Krivonos, R. A. 2013, MNRAS, 431, 327
Masetti, N., Morelli, L., Palazzi, E., et al. 2006a, A&A, 459, 21
Masetti, N., Bassani, L., Bazzano, A., et al. 2006b, A&A, 455, 11
Masetti, N., Mason, E., Morelli, L., et al. 2008, A&A, 482, 113
Masetti, N., Parisi, P., Palazzi, E., et al. 2009, A&A, 495, 121
Masetti, N., Parisi, P., Palazzi, E., et al. 2010, A&A, 519, A96
Matt, G., & Guainazzi, M. 2003, MNRAS, 341, L13
McGregor, P. J., Hyland, A. R., & Hillier, D. J. 1988, ApJ, 324, 1071
Millour, F., Meilland, A., Chesneau, O., et al. 2011, A&A, 526, A107
Mineo, S., Gilfanov, M., & Sunyaev, R. 2011, Astron. Nachr., 332, 349
Mirabel, I. F., Dijkstra, M., Laurent, P., Loeb, A., & Pritchard, J. R. 2011, A&A, 528, A149
Moon, D.-S., Kaplan, D. L., Reach, W. T., et al. 2007, ApJ, 671, L53
Morel, T., & Grosdidier, Y. 2005, MNRAS, 356, 665
Morris, P. W., Eenens, P. R. J., Hanson, M. M., Conti, P. S., & Blum, R. D. 1996, ApJ, 470, 597
Morris, D. C., Smith, R. K., Markwardt, C. B., et al. 2009, ApJ, 699, 892
Negueruela, I., & Schurch, M. P. E. 2007, A&A, 461, 631
Negueruela, I., Smith, D. M., Reig, P., Chaty, S., & Torrejón, J. M. 2006, in The X-ray Universe 2005, ed. A. Wilson, ESA SP, 604, 165
Negueruela, I., Torrejón, J. M., & McBride, V. 2007, ATel, 1239, 1
Negueruela, I., Torrejón, J. M., Reig, P., Ribó, M., & Smith, D. M. 2008, in A Population Explosion: The Nature & Evolution of X-ray Binaries in Diverse Environments, eds. R. M. Bandyopadhyay, S. Wachter, D. Gelino, & C. R. Gelino, AIP Conf. Ser., 1010, 252
Nichelli, E., Israel, G. L., Moretti, A., et al. 2011, ATel, 3205, 1
Pellizza, L. J., Chaty, S., & Negueruela, I. 2006, A&A, 455, 653
Persson, S. E., Murphy, D. C., Krzeminski, W., Roth, M., & Rieke, M. J. 1998, AJ, 116, 2475
Rahoui, F., Chaty, S., Lagage, P.-O., & Pantin, E. 2008, A&A, 484, 801
Rappaport, S., Joss, P. C., & Webbink, R. F. 1982, ApJ, 254, 616
Revnivtsev, M. G., Sazonov, S. Y., Gilfanov, M. R., & Sunyaev, R. A. 2003, Astron. Lett., 29, 587
Rodriguez, J., Tomsick, J. A., Foschini, L., et al. 2003, A&A, 407, L41
Rodriguez, J., Bodaghee, A., Kaaret, P., et al. 2006, MNRAS, 366, 274
Rodriguez, J., Tomsick, J. A., & Chaty, S. 2008, A&A, 482, 731
Rodriguez, J., Tomsick, J. A., & Chaty, S. 2009, A&A, 494, 417
Rodriguez, J., Tomsick, J. A., & Bodaghee, A. 2010, A&A, 517, A14
Romano, P., Mangano, V., Ducci, L., et al. 2012, MNRAS, 419, 2695
Romano, P., Barthelmy, S. D., D'Elia, V., et al. 2013, ATel, 4939, 1
Sana, H., de Mink, S. E., de Koter, A., et al. 2012, Science, 337, 444
Sanchez-Fernandez, C., Kuulkers, E., Bird, A. J., et al. 2009, ATel, 2194, 1
Sguera, V., Bazzano, A., Bird, A. J., et al. 2006, ApJ, 646, 452
Sguera, V., Drave, S. P., Bird, A. J., et al. 2011, MNRAS, 417, 573
Sidoli, L., Vercellone, S., Mereghetti, S., & Tavani, M. 2005, A&A, 429, L47
Sidoli, L., Mereghetti, S., Sguera, V., & Pizzolato, F. 2012, MNRAS, 420, 554
Steele, I. A., & Clark, J. S. 2001, A&A, 371, 643
Stephen, J. B., Bassani, L., Molina, M., et al. 2005, A&A, 432, L49
Swank, J. H., & Markwardt, C. B. 2004, ATel, 359, 1
Tomsick, J. A., Lingenfelter, R., Walter, R., et al. 2003, IAU Circ., 8076, 1
Tomsick, J. A., Lingenfelter, R., Corbel, S., Goldwurm, A., & Kaaret, P. 2004, ATel, 224, 1
Tomsick, J. A., Chaty, S., Rodriguez, J., et al. 2006, ApJ, 647, 1309
Tomsick, J. A., Chaty, S., Rodriguez, J., Walter, R., & Kaaret, P. 2007, ATel, 1231, 1
Tomsick, J. A., Chaty, S., Rodriguez, J., Walter, R., & Kaaret, P. 2008, ApJ, 685, 1143
Tomsick, J. A., Chaty, S., Rodriguez, J., Walter, R., & Kaaret, P. 2009, ApJ, 701, 811
Tovmassian, G., Tomsick, J. A., & Mennickent, R. 2006, ATel, 804, 1
Vercellone, S., D'Ammando, F., Striani, E., et al. 2009, ATel, 2019, 1
Walter, R., Rodriguez, J., Foschini, L., et al. 2003, A&A, 411, L427
Walter, R., Bodaghee, A., Barlow, E. J., et al. 2004, ATel, 229, 1
Walter, R., Zurita Heras, J., Bassani, L., et al. 2006, A&A, 453, 133
Wen, L., Levine, A. M., Corbet, R. H. D., & Bradt, H. V. 2006, ApJS, 163, 372
Wheelwright, H. E., de Wit, W. J., Oudmaijer, R. D., & Vink, J. S. 2012, A&A, 538, A6